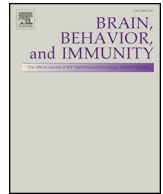




ELSEVIER

Contents lists available at ScienceDirect

## Brain, Behavior, and Immunity

journal homepage: [www.elsevier.com/locate/ybrbi](http://www.elsevier.com/locate/ybrbi)

Full-length Article

## ADAM17-deficiency on microglia but not on macrophages promotes phagocytosis and functional recovery after spinal cord injury



Daniela Sommer<sup>a</sup>, Inge Corstjens<sup>a</sup>, Selien Sanchez<sup>a</sup>, Dearbhaile Dooley<sup>b</sup>, Stefanie Lemmens<sup>a</sup>, Jana Van Broeckhoven<sup>a</sup>, Jeroen Bogie<sup>a</sup>, Tim Vanmierlo<sup>a,c</sup>, Pia M. Vidal<sup>d</sup>, Stefan Rose-John<sup>e</sup>, Myriam Gou-Fabregas<sup>a,1</sup>, Sven Hendrix<sup>a,1,\*</sup>

<sup>a</sup> Biomedical Research Institute, Hasselt University, 3500 Hasselt, Belgium<sup>b</sup> Health Science Centre, School of Medicine, University College Dublin, Dublin 4, Ireland<sup>c</sup> Division of Translational Neuroscience, MHeNs, Maastricht University, 6229ER Maastricht, the Netherlands<sup>d</sup> Laboratory of Neuroimmunology, Fundación Ciencia & Vida, 7780272 Santiago, Chile<sup>e</sup> Institute of Biochemistry, Christian-Albrechts University Kiel, 24098 Kiel, Germany

## ARTICLE INFO

## Keywords:

ADAM17

Inflammation

Macrophages

Microglia

Spinal cord injury

## ABSTRACT

A disintegrin and metalloproteinase 17 (ADAM17) is the major sheddase involved in the cleavage of a plethora of cytokines, cytokine receptors and growth factors, thereby playing a substantial role in inflammatory and regenerative processes after central nervous system trauma. By making use of a hypomorphic ADAM17 knockin mouse model as well as pharmacological ADAM10/ADAM17 inhibitors, we showed that ADAM17-deficiency or inhibition significantly increases clearance of apoptotic cells, promotes axon growth and improves functional recovery after spinal cord injury (SCI) in mice. Microglia-specific ADAM17-knockout (ADAM17<sup>flox</sup><sup>+/+</sup>-Cx3Cr1<sup>Cre</sup><sup>+/-</sup>) mice also showed improved functional recovery similar to hypomorphic ADAM17 mice. In contrast, endothelial-specific (ADAM17<sup>flox</sup><sup>+/+</sup>-Cdh5Pacs<sup>Cre</sup><sup>+/-</sup>) and macrophage-specific (ADAM17<sup>flox</sup><sup>+/+</sup>-LysM<sup>Cre</sup><sup>+/-</sup>) ADAM17-knockout mice or bone marrow chimera with transplanted ADAM17-deficient macrophages, displayed no functional improvement compared to wild type mice. These data indicate that ADAM17 expression on microglia cells (and not on macrophages or endothelial cells) plays a detrimental role in inflammation and functional recovery after SCI.

## 1. Introduction

Spinal cord injury (SCI) is characterized by a primary insult triggering a cascade of partially detrimental inflammatory processes, which aggravate initial tissue damage and impair neuronal regeneration (Beattie et al., 2002; Dooley et al., 2016; Gyoneva and Ransohoff, 2015). Microglia, the resident immune cells of the central nervous system (CNS), and infiltrating monocyte-derived macrophages are major players in this neuroinflammatory response (David et al., 2015). Microglia cells respond and enter quickly after injury, whereas monocyte-derived macrophages start entering the injured area 3 to 4 days post-injury (Orr and Gensel, 2018). Being highly plastic cells, microglia and macrophages modulate the inflammatory response by secreting pro- and anti-inflammatory cytokines and by clearing noxious factors such as apoptotic/necrotic cells (David et al., 2015; Fu et al., 2016; Graeber, 2010; Horn et al., 2008). A simplistic way to distinguish

subsets of microglia/macrophages is to divide them into *classically* and *alternatively activated* cells. *Alternatively activated* microglia/macrophages are considered to be less inflammatory due to reduced secretion of pro-inflammatory cytokines and reduced production of nitric oxide compared to *classically activated* cells (David et al., 2015).

The modulation of detrimental inflammatory processes is a major goal in SCI therapy. One key player in the modulation of inflammatory processes is 'A Disintegrin And Metalloproteinase 17' (ADAM17). ADAM17 is a membrane-bound sheddase involved in the proteolytic cleavage of not only TNF $\alpha$ , but hitherto more than 80 different known substrates including cytokines (e.g. TNF $\alpha$ ), growth factors (e.g. TGF $\alpha$ ), and multiple receptors (e.g. CSFR1) (Zunke and Rose-John, 2017). Thereby, this major sheddase affects a plethora of physiological processes during development, inflammation and tissue homeostasis as well as tissue regeneration. In neuroinflammatory pathologies, ADAM17 is playing an essential role due to the shedding of pro-

\* Corresponding author at: Martelarenlaan 42, B-3500 Hasselt, Belgium.

E-mail address: [sven.hendrix@uhasselt.be](mailto:sven.hendrix@uhasselt.be) (S. Hendrix).<sup>1</sup> Equally contributing senior authors.<https://doi.org/10.1016/j.bbi.2019.02.032>

Received 11 December 2018; Received in revised form 12 February 2019; Accepted 27 February 2019

Available online 06 March 2019

0889-1591/© 2019 The Authors. Published by Elsevier Inc. This is an open access article under the CC BY license

<http://creativecommons.org/licenses/by/4.0/>.

inflammatory mediators and the release of phagocytic receptors impairing the phagocytic capacity of phagocytes. Thereby, ADAM17 is involved in the progression of CNS pathologies as for example multiple sclerosis and traumatic brain injury (Weinger et al., 2009; Zhang et al., 2016). By using rather broad acting pharmacological inhibitors, it has been shown that ADAM17 plays an important role in the survival of glial cells and the regenerative processes after SCI (Rego et al., 2014; Vidal et al., 2013; Wei et al., 2015).

In the present study, we investigated the role of ADAM17 on functional and histological recovery after SCI. We studied i) wild type mice treated with a pharmacological ADAM10/ADAM17 inhibitor, ii) hypomorphic ADAM17<sup>ex/ex</sup> mice with a low systemic expression of ADAM17 as well as mice with a cell-type specific ADAM17 knockout on iii) endothelial cells (ADAM17<sup>flox<sup>+/+</sup></sup>-Cdh5Pacs Cre<sup>+/-</sup>), iv) microglia (ADAM17<sup>flox<sup>+/+</sup></sup>-Cx3Cr1 Cre<sup>+/-</sup>), v) macrophages (ADAM17<sup>flox<sup>+/+</sup></sup>-LysM Cre<sup>+/-</sup>) and vi) bone marrow chimeras with transplanted ADAM17-deficient macrophages.

We demonstrated that the systemic inhibition or deficiency of ADAM17 not only improves functional recovery, but also modulates immune cell infiltration and increases regeneration of serotonergic fibers after SCI. More specifically, we identified that microglia-specific ADAM17-deficiency improves functional recovery after SCI at a level similar to that observed following systemic ADAM17 inhibition or deficiency. Furthermore, we showed that in both hypomorphic ADAM17 and ADAM17<sup>flox<sup>+/+</sup></sup>-Cx3Cr1 Cre<sup>+/-</sup> transgenic mice, the phagocytic receptor CD36 was significantly upregulated and correlated with more interactions between microglia/macrophages and apoptotic cells, suggesting a favorable inflammatory response upon ADAM17-deficiency. These results suggest that the inhibition of ADAM17 may be a novel therapeutic target to promote functional and histological recovery after SCI.

## 2. Material and methods

### 2.1. Animals

Female 10-week old C57BL6/JRj mice were obtained from Janvier (France).

Hypomorphic ADAM17 mice (ADAM17<sup>ex/ex</sup>) and wild type littermates (ADAM17<sup>wt/wt</sup>) were used for *in vitro* and *in vivo* studies (Chalaris et al., 2010). ADAM17<sup>ex/ex</sup> mice express low levels of ADAM17 in all cells due to the introduction of an additional exon between exon 11 and 12 of the ADAM17 gene. The new exon starts with an in-frame stop codon but is only used inefficiently due to altered splice/donor acceptor sites resulting in < 5% ADAM17 expression as compared to wild type mice (Chalaris et al., 2010). All *in vivo* experiments with ADAM17<sup>ex/ex</sup> and ADAM17<sup>wt/wt</sup> were performed with 10- to 12-week old animals. To further investigate the effect of ADAM17 on myeloid cells, 10-week old ADAM17<sup>flox<sup>+/+</sup></sup>-LysM Cre<sup>-/-</sup> (ADAM17 MΦWT) and ADAM17<sup>flox<sup>+/+</sup></sup>-LysM Cre<sup>+/-</sup> (ADAM17 MΦKO) mice were used.

Chimeric mice were generated by whole body irradiation with 8 Gy of C57BL/6 females (Envigo, the Netherlands). Femurs and tibias were removed from female ADAM17<sup>ex/ex</sup> or female ADAM17<sup>wt/wt</sup> mice. Bone marrow was flushed with sterile PBS (phosphate buffered saline, pH: 7.5). Mice were reconstituted with 10<sup>7</sup> cells into the tail vein of recipients within 4 h post-irradiation. Bone marrow was allowed to engraft for at least 8 weeks before the mice were used for experiments. During recovery, mice were treated with Neomycin (FSA Chemicals NV, Belgium) and Polymyxini B sulfas (Fagron, the Netherlands) added to the drinking water.

ADAM17<sup>flox/flox</sup> mice (Adam<sup>tm1.2Bbl/J</sup>, ADAM17<sup>flox<sup>+/+</sup></sup>, stock 009597) were purchased from the Jackson Laboratory. Cx3Cr1 CreERT2 and Cdh5Pacs CreERT2 mice have been previously described by Prof. Dr. Steffen Jung and Prof. Dr. Ralf Adams, respectively (Wang et al., 2010; Yona et al., 2013). Mice with ADAM17-deficiency in endothelial cells (ADAM17<sup>flox<sup>+/+</sup></sup>-Cdh5Pacs Cre<sup>+/-</sup>) were obtained by breeding

ADAM17<sup>flox<sup>+/+</sup></sup> mice with transgenic Cdh5Pacs CreERT2-expressing (Cdh5Pacs Cre<sup>+/-</sup>) mice with a tamoxifen-inducible CreERT2-recombinase. For induction of Cdh5Pacs-driven Cre-recombinase, 8-week old mice were injected intraperitoneally (i.p.) 5 doses of tamoxifen (2 mg/mL; T5648, Sigma-Aldrich, Belgium) at 5 consecutive days. ADAM17<sup>flox<sup>+/+</sup></sup>-Cdh5Pacs Cre<sup>-/-</sup> mice were treated identically with tamoxifen.

Mice with ADAM17-deficiency in microglia (ADAM17<sup>flox<sup>+/+</sup></sup>-Cx3Cr1 Cre<sup>+/-</sup>) were generated by mating ADAM17<sup>flox<sup>+/+</sup></sup> mice with transgenic Cx3Cr1 CreERT2-expressing (Cx3Cr1 Cre<sup>+/-</sup>) mice with a tamoxifen-inducible CreERT2-recombinase. Induction of CreERT2-recombinase in ADAM17<sup>flox<sup>+/+</sup></sup>-Cx3Cr1 Cre<sup>+/-</sup> was achieved by administering tamoxifen (8 mg/mL) twice every other day via oral gavage at 4-weeks of age. Control littermates ADAM17<sup>flox<sup>+/+</sup></sup>-Cx3Cr1 Cre<sup>-/-</sup> also received tamoxifen.

In all experiments age- and sex-matched mice were used. Mice were housed in groups under standardized conditions with a 12-hour light-dark cycle. The mice had *ad libitum* access to food and water. All strains were kept in identical housing conditions. The experiments were performed according to the guidelines of EU Directive 2010/63/EU on the protection of animals used for scientific purposes. All experiments were approved by the local ethical committee at Hasselt University.

### 2.2. Experimental spinal cord injury

A T-cut spinal cord hemisection was performed as previously described (Boato et al., 2010; Nelissen et al., 2014; Vidal et al., 2013). Briefly, mice were anesthetized with 3% isoflurane (Isoflo, Abbot Animal Health, Belgium) and a partial laminectomy was performed at thoracic level 8 (T8). A complete transection of the dorsomedial and ventral corticospinal tract was induced bilateral dorsal T-cut hemisection using iridectomy scissors. Muscles were sutured and the back skin was closed with wound clips (Autoclip, Clay-Adams Co. Inc., US). A glucose solution (20%) was administered i.p. to compensate blood loss during surgery. As post-operative pain treatment, buprenorphine (0.1 mg/kg bodyweight Temgesic, Val d'Hony Verdifarm, Belgium) was administered subcutaneously close to the lesion site. Mice were placed in a recovery chamber (33 °C) post-surgery. Investigators remained blinded to the treatment groups for the duration of the study. Bladders of the mice were emptied daily manually until micturition reflex returned spontaneously.

For experiments with pharmacological inhibitors, animals were i.p. injected either with GI254023x (a specific ADAM10 inhibitor; 100 µg/kg; SML0789, Sigma-Aldrich), GW280264X (a selective ADAM10/ADAM17 inhibitor; 100 µg/kg; AOB3632, Aobious Inc, US) or vehicle (PBS with 0.6% DMSO) every day for one week starting 4 h post-surgery.

### 2.3. Assessment of functional recovery following spinal cord injury

Functional recovery after SCI was assessed using the Basso Mouse Scale (BMS) test (Basso et al., 2006). The BMS is a 10-point locomotor rating scale (9 = normal locomotion; 0 = complete hind limb paralysis). Mice were scored by one to two blinded investigators in an open field. During the first 8 days, mice were scored daily and afterwards only every second day. The given scores are based on hind limb movements made in an open field during a 4-min interval. The analysis was done using the mean of the left and right hind limb scores for each animal.

### 2.4. Injection of apoptotic Neuro-2a cells into the spinal cord

The Neuro-2a cell line, a murine neuroblast cell line purchased from American Type Culture Collect (CCL-131; France), was cultured in DMEM (41966-029, Gibco) medium supplemented with 10% fetal calf serum (FCS; Biochrom AG, Germany) and 1% penicillin/streptomycin

**Table 1**  
Primer sequences used for qPCR analysis.

Gene name	Forward 5'-3'	Reverse 5'-3'
ADAM17	AGAGAGCCATCTGAAGATTTGT	CTTCTCCACGGCCCATGTAT
Arginase-1	GTGAAGAACCACCGTCTGT	GCCAGAGATGCTTCCAACTG
CD163	GCTCTAGAATGGTGTACTTGAAG	CGGGATCCTCATTGTACTTCAGAGTGG
CD206	CTTCGGGCCTTTGGAATAAT	TAGAAGAGCCCTTGGGTGA
CD36	GGACATTGAGATTTCTTCTCTG	GCAAAGGCATTGGCTGGAAGAAC
CD91	GACCAGGTGTGGACACAGATG	AGTCGGTTGTCTCCGTACACACTTC
CD93	GGACGAAGAGACCTGTTG	AGATGAGTGTTCGGACGC
CYCA	GCGTCTCCTTCGAGCTGTT	AAGTCAACCACCTGGCA
GAPDH	GGCCTTCGGTGTCTCTAC	TGTCATCATATCTGGCAGGTT
HMBS	GATGGGCACTGTACCTGACTG	CTGGGCTCCTTGGAAATG
HPRT	CTCATGGACTGATTATGGACAGGAC	GCAGGTCAGCAAAGAAGCTTATAGCC
IL-1 $\beta$	ACCCTGCAGCTGGAGAGTGT	TTGACTTCTATCTTGTGAAGACAAAAC
IL-6	TGTCTATACCCTTACAAAGTCGGAG	GCACAACCTTTTCTCATTTCAC
iNOS	CCCTTCAATGGTTGGTACATGG	ACATTGATCTCCGTGACAGCC
MCP1	GGCTCAGCCAGATGCAGTTAA	AGCCTACCTCATTGGGATCATCTT
MEGF10	CCAGCCAACAGGAATGTCTAT	CTGGCAGCAGGTGATATATG
MEGF8	ACCTAGCCTCCCGTGTGTCT	ACGATCCCTGTGCGGTACA
MerTK	GTGGCAGTGAAGACCATGAAGTTG	GAACTCCGGGATAGGGAGTCAT
TNF $\alpha$	GTCCCAAAGGGATGAGAAGT	TTGTCTACGACGTGGGCTAC
TREM2	ATGGGACCTCTCCACCAGTT	TCACGTACCTCCGGGTCCA
YWHAZ	GCAACGATGTACTGTCTTTTGG	GTCACAATTCCTTCTTGTGATC

(referred to as DMEM complete). Apoptosis was induced by UV exposure at 254 nm for 15 min followed by 1 h incubation (Mazaheri et al., 2017). Cells were labelled with PKH26, a red fluorescent cell linker (PKH26MINI-1KT, Sigma-Aldrich) according to the manufacturer's instruction.

Mice were subjected to a laminectomy at T8, but no T-cut hemisection was performed. Instead a motorized stereotaxic injector pump (Stoelting, Ireland) was used as described before (Dooley et al., 2016). The needle was stereotactically inserted into the spinal cord at 4 positions at a depth of 1 mm and  $1 \times 10^4$  cells in  $1 \mu\text{L}$  of DMEM medium were injected over a time period of 1 min. The needle was subsequently kept in place for an additional minute to allow pressure equilibration and prevent backflow of the injected cells.

## 2.5. Endothelial cell isolation from adult ADAM17flox<sup>+/+</sup>-Cdh5Pacs Cre mice

Brains from tamoxifen-treated ADAM17flox<sup>+/+</sup>-Cdh5Pacs Cre<sup>+/-</sup> and control mice were isolated after cervical dislocation. All steps were performed on ice or in ice-cold solutions unless stated otherwise. The brain stem as well as meninges and blood vessels were removed. The tissue was homogenized and centrifuged (2000 rpm, 10 min, 4 °C). The cell pellet was resuspended in 15% dextran solution (Mr ~ 70 000; 31392–25, Sigma-Aldrich) and centrifuged. Afterwards the cell pellet was incubated for 30 min at 37 °C in a collagenase/dispase (2 mg/mL; 10269638001, Roche Diagnostics, Germany) with 0.01 mg/mL DNase solution (07900, Stemcell Technologies, France). After 15 min incubation with DNase (0.05 mg/mL) and centrifugation (700 g, 5 min, 4 °C), cells were stained with CD31 MicroBeads (130–097-418, Miltenyl Biotec) according to the manufacturer's instructions. CD31<sup>+</sup> cells were separated in a magnetic field using MS columns (Miltenyl Biotec). The collected cells were either lysed with RNA lysis buffer for gene expression analysis or in RIPA lysis buffer with protease (cOmplete ULTRA Tablets, 05892970001, Roche Diagnostics) and phosphatase inhibitors (PhosSTOP EASYpack, 04906837001, Roche Diagnostics) for protein analysis.

## 2.6. Microglia isolation from adult ADAM17flox<sup>+/+</sup>-Cx3Cr1 Cre mice

Microglia cells from tamoxifen-treated ADAM17flox<sup>+/+</sup>-Cx3Cr1 Cre<sup>+/-</sup> and control mice were isolated as previously described (Nikodemova and Watters, 2012). Briefly, brains were isolated after

transcardial perfusion. All steps were performed on ice unless stated otherwise. Brain stem and choroid plexus were removed from brains. After enzymatic digestion for 1 h with collagenase from *Clostridium histolyticum* (175 U/mL; C2674, Sigma-Aldrich), tissue was mechanically dissociated. After enzymatic digestion with DNase for 15 min at room temperature (RT) and centrifugation, the homogenate was resuspended in 30% isotonic Percoll (17–0891-02, GE Healthcare) and centrifuged at 700 g for 10 min. After an additional centrifugation step, the pellet was again incubated with DNase (0.05 mg/mL) in PBS. After 15 min incubation, cells were stained with CD11b MicroBeads (130–093-636, Miltenyl Biotec) according to the manufacturer's instructions. CD11b<sup>+</sup> cells were separated in a magnetic field using MS columns (Miltenyl Biotec). The collected CD11b<sup>+</sup> cells were either lysed with RNA lysis buffer or in RIPA lysis buffer.

## 2.7. RNA extraction and quantitative PCR

Mice underwent SCI surgery as described above. Mice received an overdose with Dolethal (Vetiquinol NV, Belgium) and were transcardially perfused with Ringer solution including heparin as previously described (Nelissen et al., 2014). Standardized areas of the spinal cord tissue (5 mm rostral and 5 mm caudal to the lesion center) were collected and snap frozen in liquid nitrogen. RNA was isolated using the PARIS kit (AM1921, Life Technologies, Belgium) according to the manufacturer's protocol with minor modifications as described before (Vanganswinkel et al., 2016). RNA was extracted from total cell lysates using the RNeasy Mini Kit (74104, Qiagen, the Netherlands) according to the manufacturer's instructions. After reverse transcription to cDNA using qScript cDNA Supermix (95048–100, Quanta Biosciences, US), a quantitative PCR was conducted on a StepOnePlus detection system (Applied Biosciences, Belgium) using standardized cycling conditions (20 s at 95 °C, 40 cycles of 3 s at 95 °C and 30 s at 60 °C). Primer sequences are listed in Table 1.

## 2.8. Isolation and preparation of protein samples

Protein concentration was measured in spinal cord tissue following SCI at 1, 3, 7, 14 and 28 days post-injury as described above. Mice received an overdose with Dolethal and were transcardially perfused with Ringer solution including heparin as previously described (Nelissen et al., 2014). Protein was isolated using the PARIS kit (Life Technologies) as described before (Vanganswinkel et al., 2016).

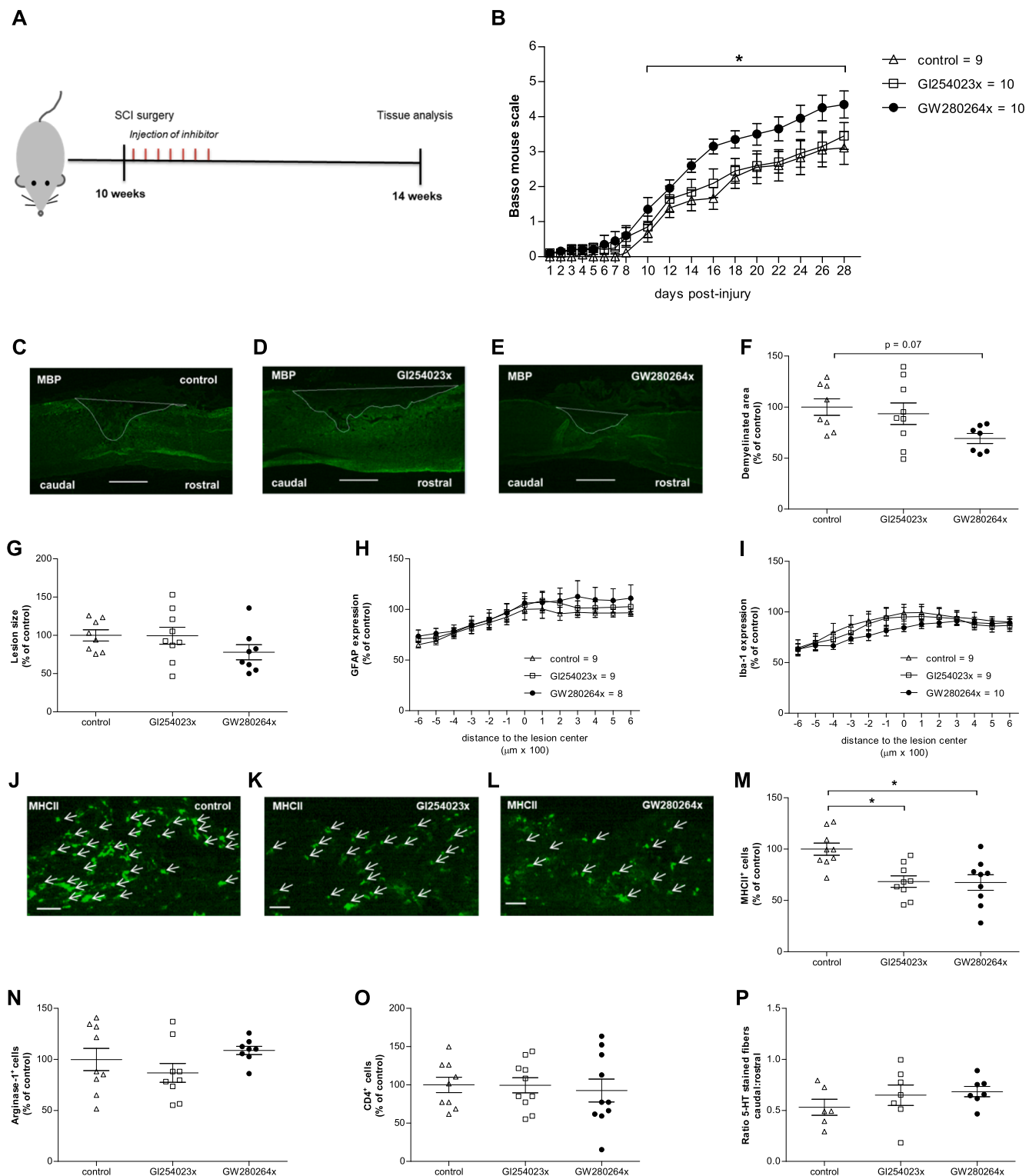
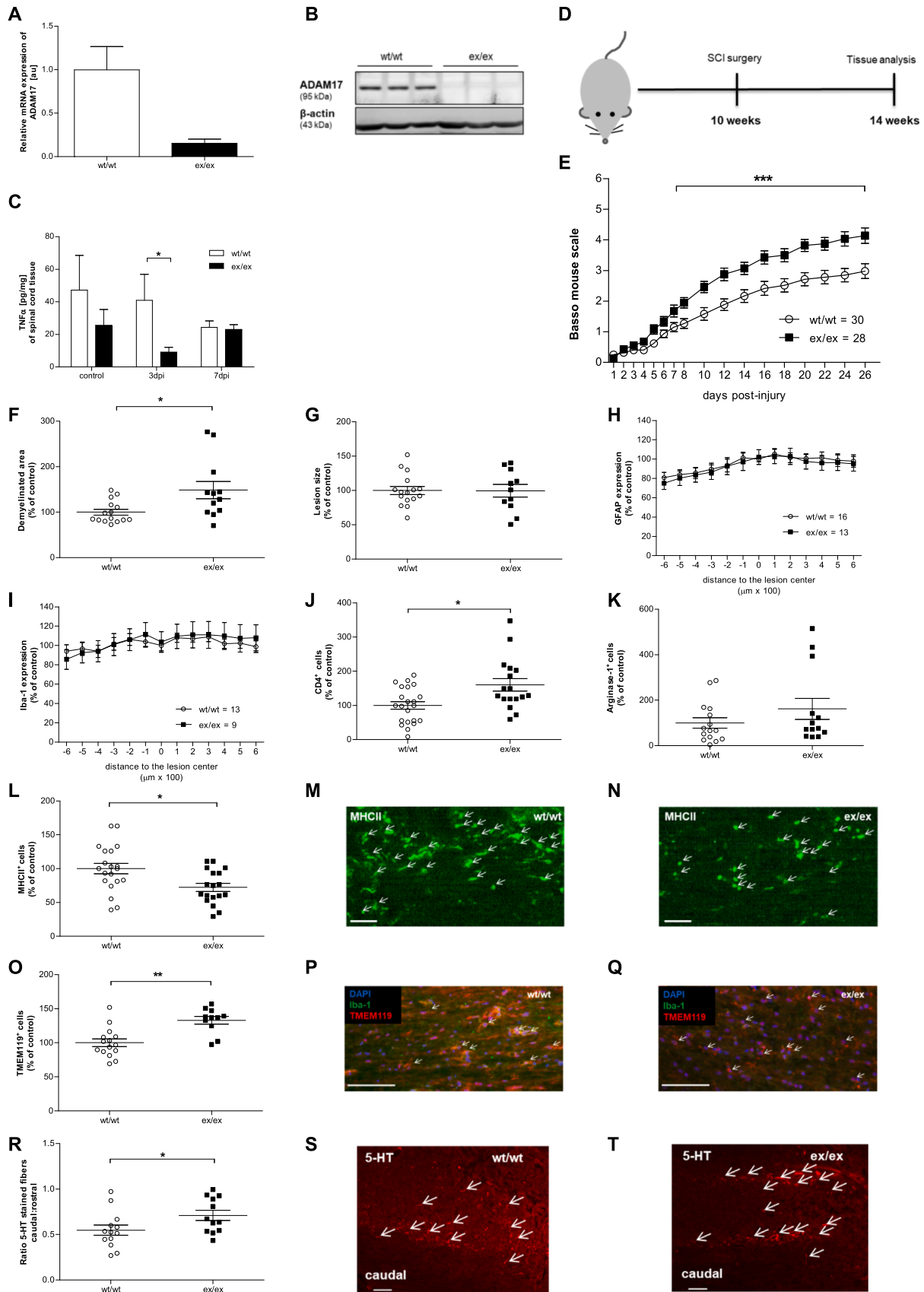


**Fig. 1.** Pharmacological inhibition of ADAM10 and ADAM17 combined, improves functional recovery and reduces the number of MHCII<sup>+</sup> cells after SCI. (A) Schematic representation of the experimental set-up. (B) Functional recovery after SCI in mice treated with GI254023x, GW280264 or control. n = 9–10 mice/group of 1 experiment; \**p* < 0.05 vs control treated group, two-way ANOVA with a Bonferroni *post-hoc* test. (C–P) Histological analyses of spinal cord sections 28 dpi. (C–E) Representative images of demyelinated area. Scale bars represent 500 μm. (F) Quantification of demyelinated area at 28 dpi. Quantification of (G) lesion size, (H) astrogliosis and (I) number of microglia/macrophages at 28 dpi. (J–L) Representative images of MHCII<sup>+</sup> cells. Scale bars represent 100 μm. Quantification of (M) MHCII<sup>+</sup> cells, (N) Arginase-1<sup>+</sup> cells and (O) CD4<sup>+</sup> T cells at 28 dpi. (P) Quantification of 5-HT<sup>+</sup> fibers at 28 dpi. n = 6–10/group; \**p* < 0.05 vs control treated group; Kruskal Wallis test with Dunn’s Multiple comparison test. Data are shown as mean ± SEM.



(caption on next page)

**Fig. 2.** ADAM17-deficiency results in a better functional recovery, modified immune cell infiltration and a greater number of serotonergic fibers after SCI. (A) ADAM17 gene expression in spinal cord tissue from ADAM17<sup>ex/ex</sup> and ADAM17<sup>wt/wt</sup> mice. n = 3/group (B) Representative immunoblot showing ADAM17 expression in spinal cord homogenates of ADAM17<sup>wt/wt</sup> and ADAM17<sup>ex/ex</sup> mice. (C) Quantification of TNF $\alpha$  levels in spinal cord homogenate from ADAM17<sup>ex/ex</sup> and ADAM17<sup>wt/wt</sup> mice at 3 and 7 dpi. Uninjured mice were used as control. n = 3–9/group, \**p* < 0.05; two-way ANOVA with a Bonferroni *post-hoc* test (D) Schematic representation of the experimental set-up. (E) Functional recovery after SCI from ADAM17<sup>ex/ex</sup> and ADAM17<sup>wt/wt</sup> mice. n = 28–30/group from 4 independent experiments. \*\*\**p* < 0.001 vs ADAM17<sup>wt/wt</sup> mice; two-way ANOVA with a Bonferroni *post-hoc* test. (F–T) Histological analysis on spinal cord sections at 28 dpi. Quantification of (F) demyelinated area, (G) lesion size, (H) astrogliosis, (I) microglia/macrophages, (J) number of CD4<sup>+</sup> T cells, (K) Arginase-1<sup>+</sup> cells and (L) MHCII<sup>+</sup> cells. (M,N) Representative images from MHCII<sup>+</sup> cells in ADAM17<sup>wt/wt</sup> and ADAM17<sup>ex/ex</sup> mice. Scale bars represent 100  $\mu$ m. (O–Q) Quantification and representative images of TMEM119<sup>+</sup> cells at 28 dpi Scale bars represent 100  $\mu$ m. (R–T) Quantification and representative images of 5-HT<sup>+</sup> fibers in ADAM17<sup>wt/wt</sup> and ADAM17<sup>ex/ex</sup> mice at 28 dpi. Scale bars represent 100  $\mu$ m. n = 11–20/group; \**p* < 0.05; \*\**p* < 0.01 vs ADAM17<sup>wt/wt</sup>, Mann Whitney *U* test. Data are shown as mean  $\pm$  SEM.

## 2.9. Cytometric bead array – cytokine/chemokine protein levels

Cytokine/chemokine protein levels were determined locally in the injured spinal cord at 3 and 7 dpi. The protein levels of pro-inflammatory cytokines were quantitatively determined via flow cytometry analysis using the mouse Cytometric Bead Array (CBA; 560485, BD Biosciences) Th1/Th2/Th17 cytokine kit according to the manufacturer's instructions and as previously described (Vanganswinkel et al., 2016).

## 2.10. Protein analysis

Western blot analysis was performed against different protein targets using protein samples isolated from spinal cords or cell lysates.

BMDM and primary microglia were collected on ice with RIPA lysis buffer with protease and phosphatase inhibitors. Total protein levels were determined using the BCA Protein Assay Kit (23227, Thermo Scientific, Belgium) according to the manufacturer's instructions. For Western blotting, equal amounts of protein samples (2–20  $\mu$ g) were electrophoretically separated and transferred onto polyvinylidene fluoride membranes (Millipore, Belgium). The membranes were blocked with 5% nonfat dry milk in tris-buffered saline (TBS) with 0.05% Tween 20 (TBST). Primary antibodies were incubated overnight at 4 °C. The following primary antibodies were used: mouse anti-Arginase-1 (sc-271430, Santa Cruz, US); rabbit anti-ADAM17 (ab2051, Abcam, United Kingdom); rabbit anti-CD91 (ab92544, Abcam); goat anti-TREM2 (ab95470, Abcam); rabbit anti-CD36 (ab133625, Abcam); rabbit anti-MEGF10 (STJ112531, St. John's Laboratory, United Kingdom); mouse anti-inducible nitric oxide synthase (iNOS; N6657, Sigma-Aldrich) and mouse anti- $\beta$ -actin (sc-47778, Santa Cruz). The membranes were incubated with secondary antibodies in 5% nonfat dry milk in TBST. The following secondary antibodies were used: goat anti-rabbit HRP (P0448, Dako, US), rabbit anti-goat HRP (P0449, Dako) and rabbit anti-mouse HRP (P0260, Dako). As a loading control,  $\beta$ -actin was used. The signal detection was performed using the ECL plus western blotting substrate (32132, Thermo Scientific). Images were taken with ImageQuant LAS 4000 Mini. Densitometric analysis was done using ImageQuant TL software.

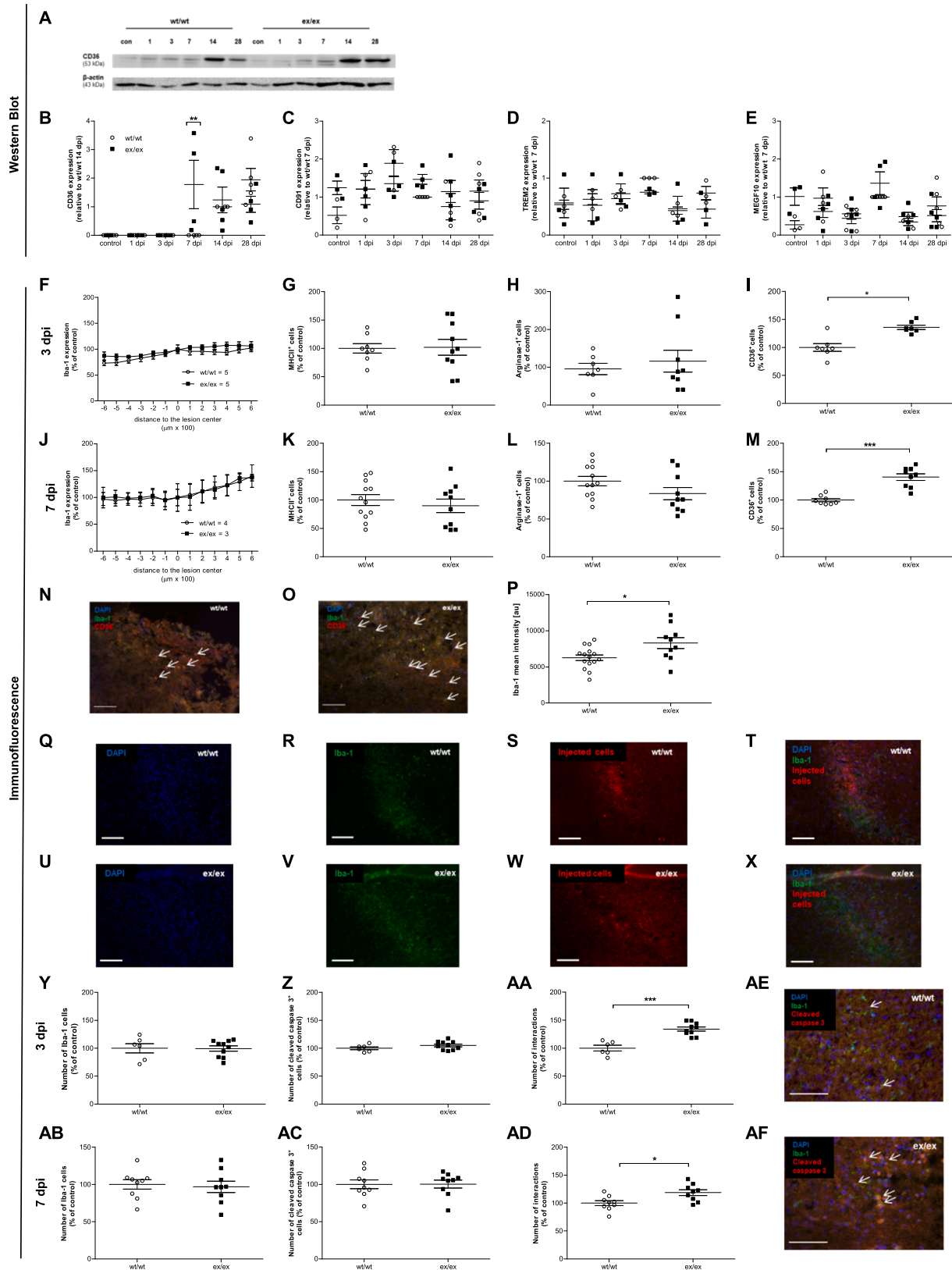
## 2.11. Immunohistochemistry

Spinal cord sections (10  $\mu$ m thick, cut serially) were obtained from experimental animals as previously described (Dooley et al., 2016). Immunofluorescence analysis was performed as previously described (Boato et al., 2010; Dooley et al., 2016; Nelissen et al., 2014; Vanganswinkel et al., 2016). To determine lesion size, demyelinated area, astrogliosis and infiltration of inflammatory cells, sections were pre-incubated with 10% protein block (X0909, Dako) containing 0.1% Triton X-100 for 1 h at RT. The following primary antibodies were incubated overnight at 4 °C: mouse anti-glial fibrillary acidic protein (GFAP; G3893, Sigma-Aldrich); rat anti-myelin basic protein (MBP; MAB386, Merck Millipore); rabbit anti-Iba-1 (019–19741, Wako; Germany); goat anti-Iba-1 (NB100-1028, Novus Biologicals, United Kingdom); rat anti-CD4 (553043, BD Biosciences, Belgium); rabbit anti-

serotonin 5-HT (20080, Acris antibodies GmbH, Germany); rabbit anti-CD36 (ab133625, Abcam); rabbit anti-TMEM119 (ab209064, Abcam) and rabbit anti-cleaved caspase 3 (96612, Bioke, the Netherlands). To determine the amount of (alternatively) activated microglia/macrophages, sections were incubated for 30 min in 0.1% Triton X-100 and afterwards treated with 10% protein block in TBS for 1 h. Primary antibodies of mouse anti-Arginase-1 (sc-271430; Santa Cruz) and rat anti-MHCII (sc-59322, Santa Cruz) were incubated overnight at 4 °C in 10% nonfat dry milk powder dissolved in TBS. The following secondary antibodies were used: goat anti-mouse Alexa Fluor 568 (A11004, Invitrogen, Belgium); goat anti-rabbit Alexa Fluor 488 (A11008, Invitrogen); goat anti-rat Alexa Fluor 568 (A11077, Invitrogen) and goat anti-rat Alexa Fluor 488 (A11006, Invitrogen). Tissue sections were counterstained with DAPI for 10–15 min. Afterwards sections were mounted using fluorescence anti-fade mounting medium (S3032, Dako). Analysis of immunofluorescence labelling was performed using a Nikon eclipse 80i microscope and NIS Elements Viewer 4. Software was used for further processing of images.

## 2.12. Quantitative image analysis

For measurement of lesion size and demyelinated area, 4–7 sections per animal containing the lesion center as well as consecutive rostral and caudal areas were analyzed. Lesion size (GFAP immunofluorescence), demyelinated area (MBP immunofluorescence), astrogliosis (GFAP expression) and microglia/macrophage activation (Iba-1 expression) were analyzed as previously described (Dooley et al., 2016; Vanganswinkel et al., 2016). All images were acquired at once and microscope settings remained the same for all the images. To quantify (alternatively) activated microglia/macrophages at the lesion site, the number of positive cells was counted on sections stained against MHCII and Arginase-1. CD4<sup>+</sup> T cells were identified through a double labelling against CD4 and Iba-1 to exclude possible CD4<sup>+</sup> microglia cells. The number of CD4<sup>+</sup> T cells was counted throughout the entire spinal cord section as previously described (Dooley et al., 2016). The mean number of TMEM119<sup>+</sup> cells counted rostral and caudal to lesion was calculated per animal. To quantify CD36 expression on microglia/macrophages, a double labelling against Iba-1 and CD36 was performed. The mean number of CD36/Iba-1<sup>+</sup> – cells counted rostral and caudal to lesion site was calculated per animal. Quantification of microglia/macrophage interactions with apoptotic cells was performed doing a double labelling for Iba-1 and cleaved caspase 3 (a well-known marker for apoptosis). An interaction was defined as the formation of a contact of microglial/macrophage processes or the formation of a microglia/macrophage pouch with an apoptotic cell (Abiega et al., 2016). The mean number of interactions between Iba-1<sup>+</sup> and cleaved caspase 3<sup>+</sup> cells determined rostral and caudal to the lesion was calculated per animal. Quantification of microglia/macrophage and axon interactions was performed by counting the number of contacts between neurofilament<sup>+</sup> dystrophic axon bulbs and Iba-1<sup>+</sup> microglia/macrophages. Dystrophic axonal bulbs were identified based on their globular and bulbous morphology extending from an axon fiber. A contact was determined when a cell–cell interaction was observed between a dystrophic axonal bulb and an Iba-1<sup>+</sup> cell which contained a DAPI<sup>+</sup>



(caption on next page)

nucleus. Analysis was performed in two standardized areas rostral and caudal from the lesion epicenter and the mean number of contacts in these two areas was calculated per animal as previously described (Dooley et al., 2016). For analysis of serotonergic fibers, sections were stained for 5-HT as described previously (Boato et al., 2010). The total

fiber length was assessed caudal and rostral to the lesion using ImageJ open source software. The mean ratio of 5-HT<sup>+</sup> fibers caudal and rostral to the lesion was calculated per animal.

**Fig. 3.** ADAM17-deficiency increases CD36 expression levels and the number of cellular interactions between Iba-1<sup>+</sup> microglia/macrophages and apoptotic cells after SCI. (A) Representative immunoblot showing CD36 expression in spinal cord homogenates after 1, 3, 7, 14 and 28 dpi. Protein expression of (B) CD36, (C) CD91, (D) TREM2 and (E) MEGF10.  $n = 3\text{--}5/\text{group}$ ,  $^{**}p < 0.01$  two-way ANOVA with a Bonferroni *post-hoc* test. (Quantification of (F, J) Iba-1, (G, K) MHCII<sup>+</sup> cells, (H, L) Arginase-1<sup>+</sup> cells and (I, M) CD36/Iba-1<sup>+</sup> cells in spinal cord tissue at 3 and 7 dpi.  $n = 3\text{--}12/\text{group}$  of 2 independent experiments,  $^{*}p < 0.05$ ;  $^{***}p < 0.001$  vs ADAM17<sup>wt/wt</sup>, Mann Whitney *U* test. (N, O) Representative images from ADAM17<sup>wt/wt</sup> and ADAM17<sup>ex/ex</sup> mice showing CD36/Iba-1 stained sections at 3 dpi. Scale bars represent 100  $\mu\text{m}$ . (P–X) Quantification and representative images of Iba-1 intensity at the injection site of PKH26-labelled apoptotic cells in uninjured ADAM17<sup>ex/ex</sup> and ADAM17<sup>wt/wt</sup> mice. Scale bars represent 100  $\mu\text{m}$ .  $n = 10\text{--}15/\text{injection sites per group}$ ,  $^{*}p < 0.05$  vs ADAM17<sup>wt/wt</sup>, Mann Whitney *U* test. (Y–AF) Quantification of (Y, AB) Iba-1<sup>+</sup> cells, (Z, AC) cleaved caspase 3<sup>+</sup> cells and (AA, AD) microglia/macrophage-cleaved caspase 3 interactions at 3 and 7 dpi in ADAM17<sup>ex/ex</sup> and ADAM17<sup>wt/wt</sup> mice. (AE, AF) Representative images from Iba-1 and cleaved caspase 3 stained sections. Scale bars represent 100  $\mu\text{m}$ .  $n = 6\text{--}10/\text{group}$  of 2 independent experiments.  $^{*}p < 0.05$ ,  $^{***}p < 0.001$  vs ADAM17<sup>wt/wt</sup>; Mann Whitney *U* test. Data are shown as mean  $\pm$  SEM.

### 2.13. Differentiation and stimulation of bone marrow-derived macrophages for *in vitro* studies

Bone marrow was isolated as described above. Cell suspension was dispersed and cultured with RPMI 1640 (BE12-115F/U1, Lonza) supplemented with 10% FCS, penicillin (100 U/mL), streptomycin (100  $\mu\text{g}/\text{mL}$ ) (referred to as RPMI complete) and 15% of L929 cell conditioned medium (LCM) containing M-CSF. Cells were maintained in humidified incubators at 37 °C with 5% CO<sub>2</sub> in air atmosphere. BMDM were harvested after 10 days and were seeded in 24-well plates (Greiner) at a density of  $2 \times 10^5$  cells. Cells were treated with a respective stimulus (0.2  $\mu\text{g}/\text{mL}$  of Lipopolysaccharide from *E. coli* 055:B5 (LPS; 437625, MERCK, Germany); 0.1  $\mu\text{g}/\text{mL}$  of interferon  $\gamma$  (IFN $\gamma$ ; Peprotech); 0.033  $\mu\text{g}/\text{mL}$  of interleukin-4 (IL-4; Peprotech). After 24 h or 48 h, conditioned medium was collected and samples were collected for gene or protein analysis, respectively.

### 2.14. Isolation and stimulation of microglia cells for *in vitro* studies

Primary microglia cultures were prepared from postnatal P0-P3 pups derived from ADAM17<sup>wt/wt</sup> and ADAM17<sup>ex/ex</sup> mice as previously described (Tamashiro et al., 2012). The tissue was dissociated in DMEM complete. Cell suspension was seeded per T75 culture flask. Cells were maintained in humidified incubators at 37 °C with 5% CO<sub>2</sub> in air atmosphere. After reaching 80% confluency, DMEM complete containing 1/3 LCM was added. Microglia cells were isolated 6–7 days later using the shake-off method (200 rpm, 2 h, 37 °C). Microglia were seeded in 24-well plates at a density of  $2 \times 10^5$  cells per well in 2/3 DMEM complete and 1/3 LCM 24 h prior to stimulation. Cells were treated with a respective stimulus (0.2  $\mu\text{g}/\text{mL}$  of LPS; 0.1  $\mu\text{g}/\text{mL}$  of IFN $\gamma$ ; 0.033  $\mu\text{g}/\text{mL}$  of IL-4) for 24 h or 48 h. After 24 h or 48 h, conditioned medium was collected and samples were collected for gene or protein analysis, respectively.

### 2.15. Nitrite formation

The nitrite concentration in conditioned medium was measured using the Griess reagent system kit (G2930 Promega).

### 2.16. *In vitro* phagocytosis assays

BMDM or microglia isolated from ADAM17<sup>ex/ex</sup> mice and wild type littermates were seeded in a 24-well plate at a density of  $2 \times 10^5$  cells per well in RPMI complete supplemented with 15% LCM or DMEM complete. After 24 h, cells were treated with a respective stimulus (0.2  $\mu\text{g}/\text{mL}$  of LPS; 0.1  $\mu\text{g}/\text{mL}$  of IFN $\gamma$ ; 0.033  $\mu\text{g}/\text{mL}$  of IL-4). After overnight incubation DiI-labelled apoptotic Neuro-2a cells (ratio 4:1) (Wagner et al., 2011) were added to the cells. After 90 min, the cells were washed with PBS and collected in FACS buffer (1  $\times$  PBS supplemented with 2% FCS and 0.1% sodium azide). The amount of phagocytosed DiI-labelled apoptotic cells was determined using the FACS Fortessa (BD Biosciences).

### 2.17. Statistical analysis

All statistical analyses were performed using GraphPad Prism 5.01 software (GraphPad Software Inc., US). Functional recovery *in vivo* and histological analyses of astrogliosis and Iba-1 intensity were statistically analyzed using two-way ANOVA for repeated measurements following Bonferroni *post-hoc* test. Differences between three groups were evaluated using a Kruskal Wallis test following Dunn's multiple comparison test. Differences between two groups were analyzed using the non-parametric Mann Whitney *U* test. For *in vivo* and *in situ* studies,  $n$  values refer to the number of mice. A  $p$  value of  $< 0.05$  was considered to be statistically significant. Data in graphs are presented as mean  $\pm$  standard error of the mean (SEM) unless otherwise stated.

## 3. Results

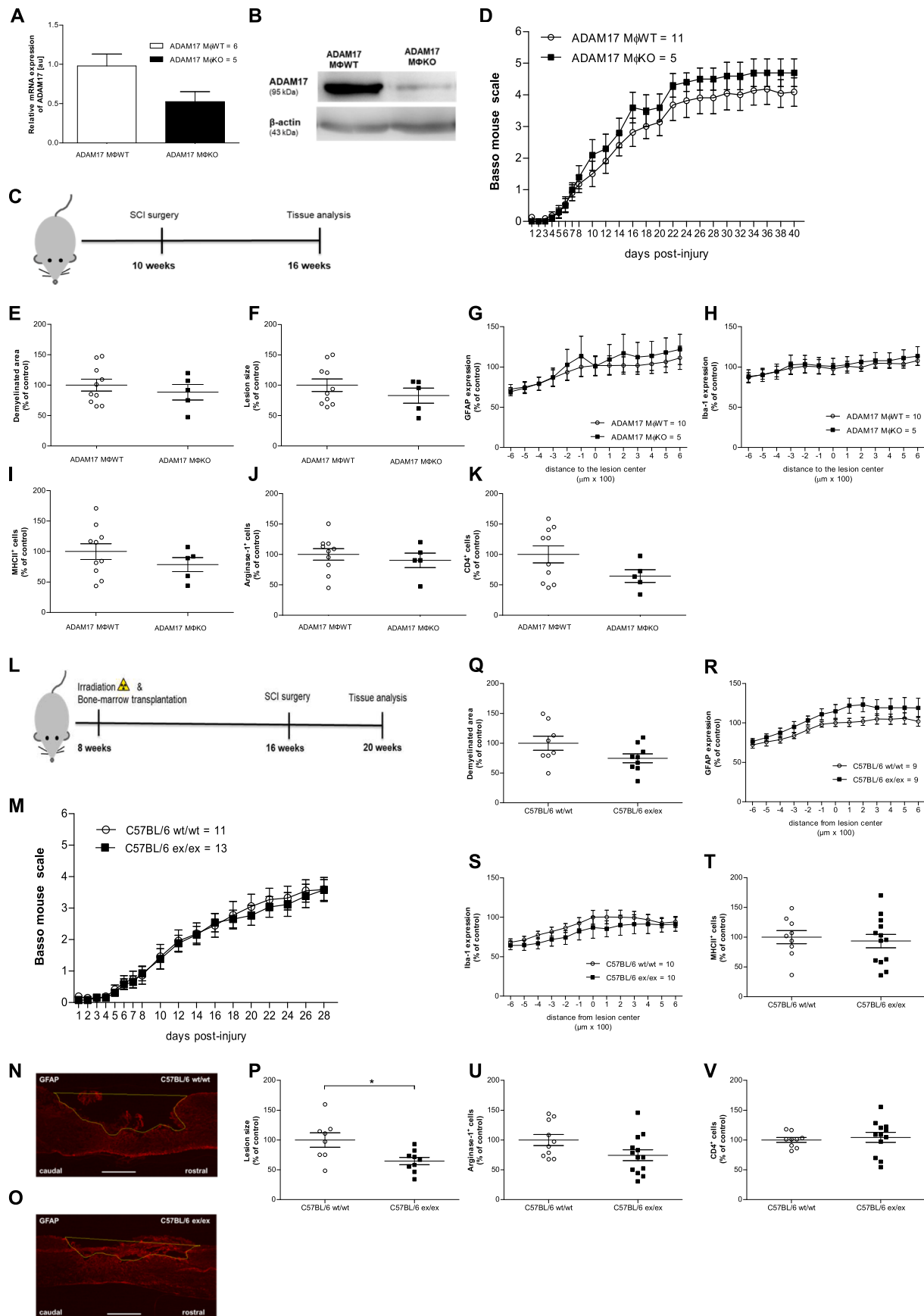
### 3.1. Pharmacological inhibition of ADAM10 and ADAM17 improves functional recovery and reduces the number of MHCII<sup>+</sup> cells after SCI

Due to the sequence homology between ADAM10 and ADAM17 and their shared substrates (Drey Mueller and Ludwig, 2017), we investigated whether ADAM10 and/or ADAM17 can modulate functional and histological recovery after SCI. To do so, we followed an indirect strategy using a specific ADAM10 and a combined ADAM10/ADAM17 pharmacological inhibitor (Hundhausen et al., 2003). C57BL/6 mice were subjected to SCI and were treated either with GW280264x (combined ADAM10/ADAM17 inhibition), GI254023x (specific ADAM10 inhibition), or PBS + DMSO (control) (Fig. 1A). Mice treated with GW280264x showed significantly improved functional recovery compared to the control group (Fig. 1B). In contrast, inhibition of ADAM10 alone had no significant effect on functional recovery compared to control treated mice (Fig. 1B).

A trend towards a decreased demyelinated area in GW280264x compared to control mice was observed (Fig. 1C–E), whereas no difference was observed between GI254023x and control treated groups (Fig. 1F). There was no difference in lesion size, astrogliosis and microglia/macrophages (Fig. 1G–I) in GI254023x, GW280264x and control treated mice. However, there was a significant decrease in the number of MHCII<sup>+</sup> cells in mice treated with GI254023x and GW280264x compared to controls (Fig. 1J–M). No difference was observed in the number of Arginase-1<sup>+</sup> cells or CD4<sup>+</sup> T cells in GI254023x or GW280264x compared to control treated mice (Fig. 1N–O). Furthermore, there was no difference in the ratio of 5-HT<sup>+</sup> fibers between the 3 groups (Fig. 1P). Taken together, these results indicate that the combined pharmacological inhibition of ADAM10/ADAM17/ADAM10/ADAM17 reduces the number of MHCII<sup>+</sup> cells and improves functional recovery following SCI suggesting that ADAM17 is responsible for these effects.

### 3.2. ADAM17-deficiency leads to a significantly improved functional recovery, accompanied with an altered immune cell infiltration and an increase in serotonergic fibers after SCI

To ensure that the above described effects with the selective ADAM10/ADAM17 inhibitor are due to the specific inhibition of



(caption on next page)

**Fig. 4.** ADAM17-deficiency on myeloid cells does not affect functional recovery and immune cell infiltration after SCI. (A) ADAM17 gene expression levels from BMDM of ADAM17 MΦWT and ADAM17 MΦKO mice. Values were converted to fold change values vs ADAM17 MΦWT.  $n = 5–6$ /group. Data are shown as mean  $\pm$  SD. (B) Representative immunoblot showing ADAM17 knockdown efficiency in BMDM isolated from ADAM17 MΦWT and ADAM17 MΦKO mice. (C) Schematic representation of the experimental set-up. (D) Functional recovery after SCI from ADAM17 MΦKO and ADAM17 MΦWT.  $n = 5–11$ /group of 1 experiment. Graph bars represent SEM. Quantification of (E) demyelinated area, (F) lesion size, (G) astrogliosis, (H) microglia/macrophages, (I) MHCII<sup>+</sup> cells, (J) Arginase-1<sup>+</sup> cells and (K) CD4<sup>+</sup> T cells in spinal cord sections at 40 dpi.  $n = 5–10$ /group. Graph bars represent SEM. (L) Schematic representation of the experimental set-up. (M) Functional recovery after SCI of C57BL/6 ex/ex and C57BL/6 wt/wt mice.  $n = 11–13$ /group. Graph bars represent SEM. (N–P) Representative images and quantification of lesion size. Scale bars represent 500  $\mu$ m. Quantification of (Q) demyelinated area, (R) astrogliosis, (S) microglia/macrophages, (T) MHCII<sup>+</sup> cells, (U) Arginase-1<sup>+</sup> cells and (V) CD4<sup>+</sup> T cells in at 28 dpi in C57BL/6 ex/ex and C57BL/6 wt/wt mice.  $n = 8–13$ /group, \* $p < 0.05$  vs C57BL/6 wt/wt; Mann Whitney U test. Data are shown as mean  $\pm$  SEM.

ADAM17, we used hypomorphic ADAM17 mice. Unlike mice with a systemic ADAM17 knockout, hypomorphic ADAM17 mice are viable (Chalaris et al., 2010).

The knockdown of ADAM17 was confirmed on gene (Fig. 2A) and protein level (Fig. 2B). In order to confirm the functional effects of ADAM17 knockdown, the levels of the ADAM17 substrate, TNF $\alpha$ , were analyzed in spinal cords isolated at 3 and 7 dpi. There was a significant decrease at 3 dpi in TNF $\alpha$  in spinal cords of hypomorphic ADAM17<sup>ex/ex</sup> mice compared to wild type littermates (ADAM17<sup>wt/wt</sup>) (Fig. 2C). To further investigate whether ADAM17-deficiency does lead to a better functional recovery after SCI, ADAM17<sup>ex/ex</sup> and control mice were subjected to a T-cut hemisection and functional recovery was assessed for 28 days using the BMS (Fig. 2D). ADAM17<sup>ex/ex</sup> mice displayed a significantly improved functional recovery compared with wild type mice (Fig. 2E).

Quantification of demyelinated area at 28 dpi revealed a significant increase in ADAM17<sup>ex/ex</sup> mice compared to wild type littermates (Fig. 2F). There was no difference in lesion size, astrogliosis and microglia/macrophages presence (Fig. 2G–I) in ADAM17<sup>ex/ex</sup> mice compared to wild type controls. Quantification of CD4<sup>+</sup> T cells throughout the spinal cord revealed a significant increase in ADAM17<sup>ex/ex</sup> mice compared to wild type littermates (Fig. 2J). While there was no difference in the number of Arginase-1<sup>+</sup> cells (Fig. 2K), a significant reduction in the number of MHCII<sup>+</sup> cells at the lesion site was determined in ADAM17<sup>ex/ex</sup> compared to wild type mice (Fig. 2L–N). Further analysis *in vitro* revealed that ADAM17-deficiency does not lead to a consistent phenotype switch in bone marrow-derived macrophages and primary microglia (supplementary Fig. S1). The number of TMEM119<sup>+</sup> microglia cells was significantly increased in ADAM17<sup>ex/ex</sup> mice compared to controls (Fig. 2O–Q). ADAM17<sup>ex/ex</sup> mice displayed a significant increase in the ratio of 5-HT<sup>+</sup> fibers compared to wild type littermates (Fig. 2R–T). We further investigated whether ADAM17-deficiency affects axonal dieback and counted therefore the number of microglia/macrophage-axon interactions using Iba-1 and neurofilament staining (Supplementary Fig. S2A). No difference in the number of microglia/macrophage-axon contacts between ADAM17<sup>ex/ex</sup> and wild type littermates was observed.

### 3.3. ADAM17-deficiency increases apoptotic receptor CD36 expression levels and Iba-1-apoptotic cell interactions after SCI

The data provided above demonstrate that ADAM17-deficiency leads to an improved functional recovery after SCI. In addition, ADAM17-deficiency may increase the number of microglia cells and alter the inflammatory environment by reducing levels of soluble TNF $\alpha$  and the number of MHCII<sup>+</sup> cells. As professional phagocytes, microglia and macrophages play an important role in the resolution of inflammation. Since ADAM17 affects the expression levels of several phagocytic receptors, we investigated whether ADAM17-deficiency influences phagocytosis after SCI.

We investigated gene expression levels of selected phagocytic receptors in ADAM17<sup>ex/ex</sup> and wild type control mice sacrificed at 1, 3 and 7 dpi. Gene expression analysis of pro- and anti-inflammatory cytokines revealed no clear differences between ADAM17<sup>ex/ex</sup> mice and wild type littermates (Suppl. Fig. S3). CD36 expression levels were

significantly increased at 7 dpi in ADAM17<sup>ex/ex</sup> mice compared to wild type littermates (Suppl. Fig. S4A). CD91, TREM2 and Megf10 gene expression levels were significantly increased at 3 dpi in ADAM17<sup>ex/ex</sup> compared to wild type control mice (Suppl. Fig. S4B–D), whereas no significant differences were observed in the expression of CD163, MerTK, CD93 and Megf8 (Supplementary Fig. S4E–H). Next, we investigated protein expression levels in the receptors which showed a significant change on gene expression after SCI. Western blotting revealed a significant increase in CD36 expression at 7 dpi in ADAM17<sup>ex/ex</sup> compared to wild type mice (Fig. 3A and B). No significant differences were determined in CD91, TREM2 and MEGF10 levels (Fig. 3C–E).

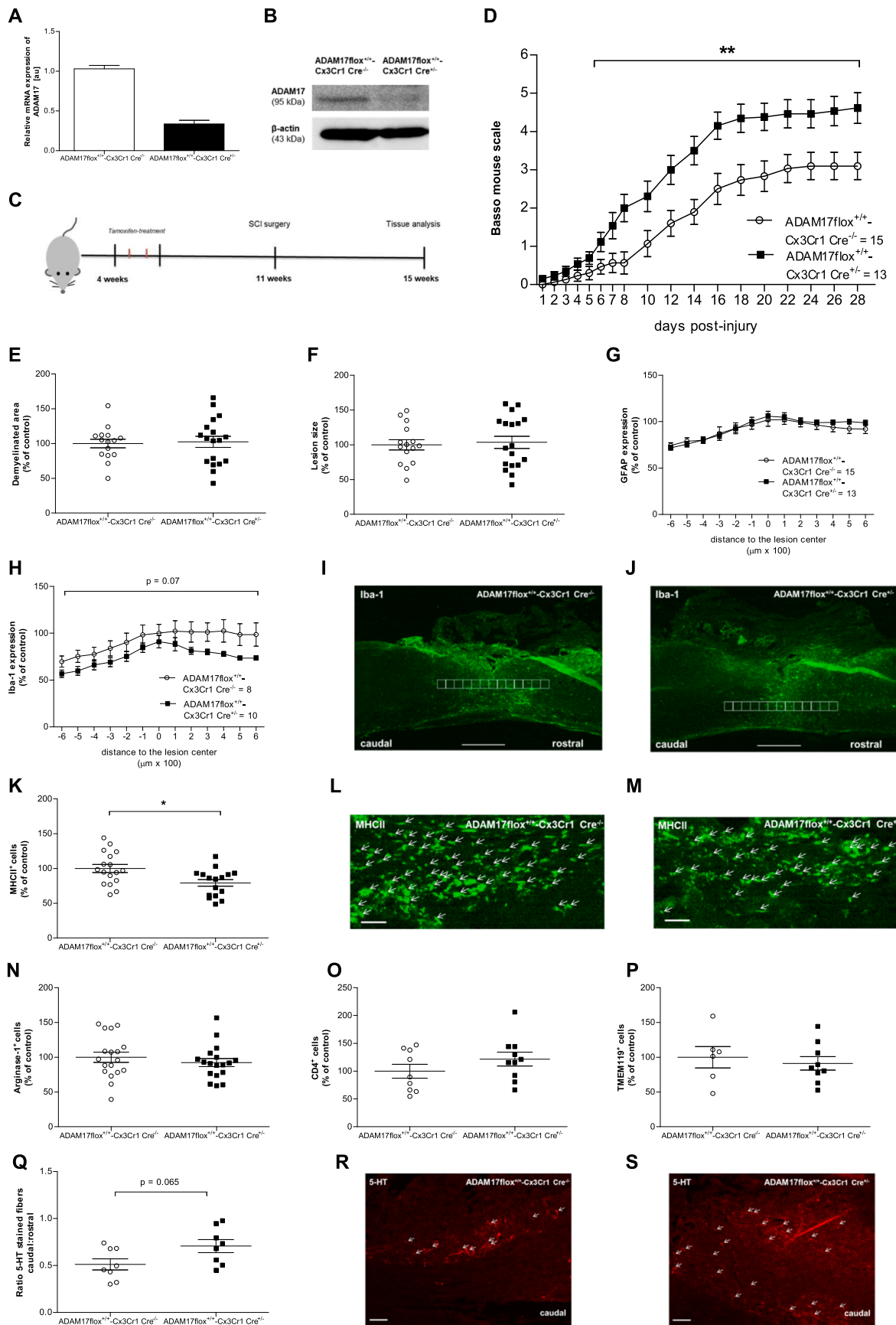
Histological analysis revealed no differences in Iba-1 expression and in the number of MHCII<sup>+</sup> and Arginase-1<sup>+</sup> cells between ADAM17<sup>ex/ex</sup> mice and wild type littermates (Fig. 3F, J, G–H, K–L). Quantification of CD36/Iba-1 double positive cells revealed an increase in numbers of CD36<sup>+</sup> microglia/macrophages in ADAM17<sup>ex/ex</sup> mice compared to wild type controls (Fig. 3I, M–O).

To test whether ADAM17-deficiency affects migration and phagocytosis of Iba-1<sup>+</sup> cells, we injected apoptotic neurons into the spinal cord of ADAM17<sup>ex/ex</sup> mice and wild type littermates. Apoptotic cells play a detrimental role during secondary injury after SCI and are known to release so-called “find-me” signals which can attract professional phagocytes (David et al., 2015; Ravichandran, 2010). Histological analysis revealed a significantly higher Iba-1 intensity at the injection site in ADAM17<sup>ex/ex</sup> compared to wild type mice (Fig. 3P–X).

Increased CD36 expression on phagocytes (Fig. 3I, M–O) may indicate increased clearance of apoptotic cells. Therefore, we investigated the interaction of microglia/macrophages with apoptotic cells using Iba-1 and cleaved caspase 3 double labelling. While the number of Iba-1<sup>+</sup> microglia/macrophages and cleaved caspase 3<sup>+</sup> cells were similar between the groups, the number of microglia/macrophage-apoptotic cell interactions was significantly increased at 3 and 7 dpi in ADAM17<sup>ex/ex</sup> mice compared to wild type littermates (Fig. 3Y–AF). Furthermore, *in vitro* analysis with ADAM17-deficient macrophages and microglia cells revealed a trend towards a better phagocytic capacity of apoptotic cells by ADAM17-deficient BMDM and a significantly higher phagocytic capacity of apoptotic cells by ADAM17-deficient microglia upon IL-4 stimulation (Suppl. Fig. S5). Taken together, these results indicate that ADAM17-deficiency leads to a significant increase in phagocytic receptor expression, particularly CD36, and the interaction of microglia/macrophages with apoptotic cells after SCI.

### 3.4. ADAM17-deficiency on myeloid cells does not lead to a better functional recovery and does not affect immune cell infiltration after SCI

Overall, the results provided so far suggest that ADAM17 plays a detrimental role in functional recovery after SCI. Since immune cell infiltration and activation were altered in ADAM17-deficient mice after SCI (Fig. 2) and given that ADAM17 is a ubiquitously expressed protease, we further investigated the effect of ADAM17-deficiency on specific cell types. Due to the effect of ADAM17 on barrier function, we investigated the effect of ADAM17-deficiency on endothelial cells. Our results strongly indicate that endothelial-specific ADAM17-deficiency does not affect functional recovery and immune cell infiltration



(caption on next page)

**Fig. 5.** Microglia-specific ADAM17-deficiency improves functional recovery and reduces the number of MHCII<sup>+</sup> cells after SCI. (A) ADAM17 gene expression levels in *ex vivo* microglia isolated from ADAM17<sup>+/+</sup>-Cx3Cr1 Cre<sup>+/-</sup> and control mice after tamoxifen administration. Data are shown as mean ± SD. n = 6–14/group from 2 independent experiments. (B) Representative immunoblot showing ADAM17 knockdown efficiency in *ex vivo* microglia cells isolated from ADAM17<sup>+/+</sup>-Cx3Cr1 Cre<sup>+/-</sup> and control mice. (C) Schematic representation of the experimental set-up. (D) Functional recovery of ADAM17<sup>+/+</sup>-Cx3Cr1 Cre<sup>+/-</sup> and ADAM17<sup>+/+</sup>-Cx3Cr1 Cre<sup>-/-</sup> mice after SCI. n = 13–15/group one representative graph from 1 of 2 independent *in vivo* experiments. \*\*p < 0.01 vs ADAM17<sup>+/+</sup>-Cx3Cr1 Cre<sup>-/-</sup> mice; two-way ANOVA with Bonferroni *post-hoc* test. Graph bars represent SEM. Quantification of (E) demyelinated area, (F) lesion size, (G) astrogliosis and (H) microglia/macrophages in ADAM17<sup>+/+</sup>-Cx3Cr1 Cre<sup>+/-</sup> mice and control mice. (I–J) Representative images of Iba-1 stained spinal cord sections. Scale bar 500 μm. (K–M) Quantification and representative images of MHCII<sup>+</sup> cells in ADAM17<sup>+/+</sup>-Cx3Cr1 Cre<sup>+/-</sup> mice compared to ADAM17<sup>+/+</sup>-Cx3Cr1 Cre<sup>-/-</sup> mice at 28 dpi. n = 16–17/group, \*p < 0.05 vs ADAM17<sup>+/+</sup>-Cx3Cr1 Cre<sup>-/-</sup>; Mann Whitney U test. Graph bars represent SEM. Quantification of (N) Arginase-1<sup>+</sup> cells, (O) CD4<sup>+</sup> T cells and (P) TMEM119<sup>+</sup> cells. Graph bars represent SEM. (Q–S) Quantification of regenerated 5-HT<sup>+</sup> fibers from ADAM17<sup>+/+</sup>-Cx3Cr1 Cre<sup>-/-</sup> and ADAM17<sup>+/+</sup>-Cx3Cr1 Cre<sup>+/-</sup> mice. Scale bars represent 100 μm. n = 8/group, \*p < 0.05 vs ADAM17<sup>+/+</sup>-Cx3Cr1 Cre<sup>-/-</sup>; Mann Whitney U test. Data are shown as mean ± SEM.

following SCI (Suppl. Fig. S6).

In order to investigate whether ADAM17-deficiency specifically on myeloid cells leads to a better functional recovery after SCI, we crossed mice carrying a floxed ADAM17 allele (ADAM17<sup>+/+</sup>) with LysM Cre transgenic mice expressing Cre-recombinase under the control of the LysM-promoter. This promoter is mainly expressed in myeloid cells, and thus, we compared ADAM17<sup>+/+</sup>-LysM Cre<sup>+/-</sup> (ADAM17 MΦKO) with ADAM17<sup>+/+</sup>-LysM Cre<sup>-/-</sup> (ADAM17 MΦWT) mice (Clausen et al., 1999; Horiuchi et al., 2007). To confirm the knockdown efficiency in this mouse line, we determined ADAM17 mRNA expression (Fig. 4A) and protein levels (Fig. 4B) in BMDM isolated from ADAM17 MΦWT and ADAM17 MΦKO mice. Functional recovery after SCI was assessed (Fig. 4C). No difference in functional recovery in ADAM17 MΦKO compared to ADAM17 MΦWT mice was observed (Fig. 4D). Histological analysis also revealed no differences in demyelinated area, lesion size, astrogliosis and the number of microglia/macrophages, MHCII<sup>+</sup>, Arginase-1<sup>+</sup> or CD4<sup>+</sup> T cells in ADAM17 MΦKO compared to ADAM17 MΦWT mice (Fig. 4E–K). Although the LysM Cre system is widely used to study myeloid-specific deletions, it is well-known to be highly variable in its deletion efficiency (Murray and Wynn, 2011). Thus, to provide further evidence that ADAM17-deficiency on myeloid cells is *not* responsible for the beneficial effects of ADAM17 reduction in ADAM17<sup>ex/ex</sup> mice, we transplanted ADAM17<sup>ex/ex</sup> or ADAM17<sup>wt/wt</sup> bone marrow into irradiated C57BL/6 mice. Functional recovery of recipients of ADAM17<sup>ex/ex</sup> (C57BL/6 ex/ex) and ADAM17<sup>wt/wt</sup> (C57BL/6 wt/wt) bone marrow was assessed (Fig. 4L). There was no difference observed in functional recovery between the two groups (Fig. 4M). Quantification of the lesion size revealed a significant decrease in C57BL/6 ex/ex compared to C57BL/6 wt/wt mice (Fig. 4N–P). Further histological analysis revealed no differences in demyelinated area, astrogliosis, microglia/macrophages and in the number of MHCII<sup>+</sup>, Arginase-1<sup>+</sup> or CD4<sup>+</sup> T cells (Fig. 4Q–V). Together, these results indicate that ADAM17-deficiency on myeloid cells does not significantly affect functional recovery and immune cell infiltration after SCI.

### 3.5. Microglia-specific ADAM17-deficiency improves functional recovery and reduces the number of MHCII<sup>+</sup> cells after SCI

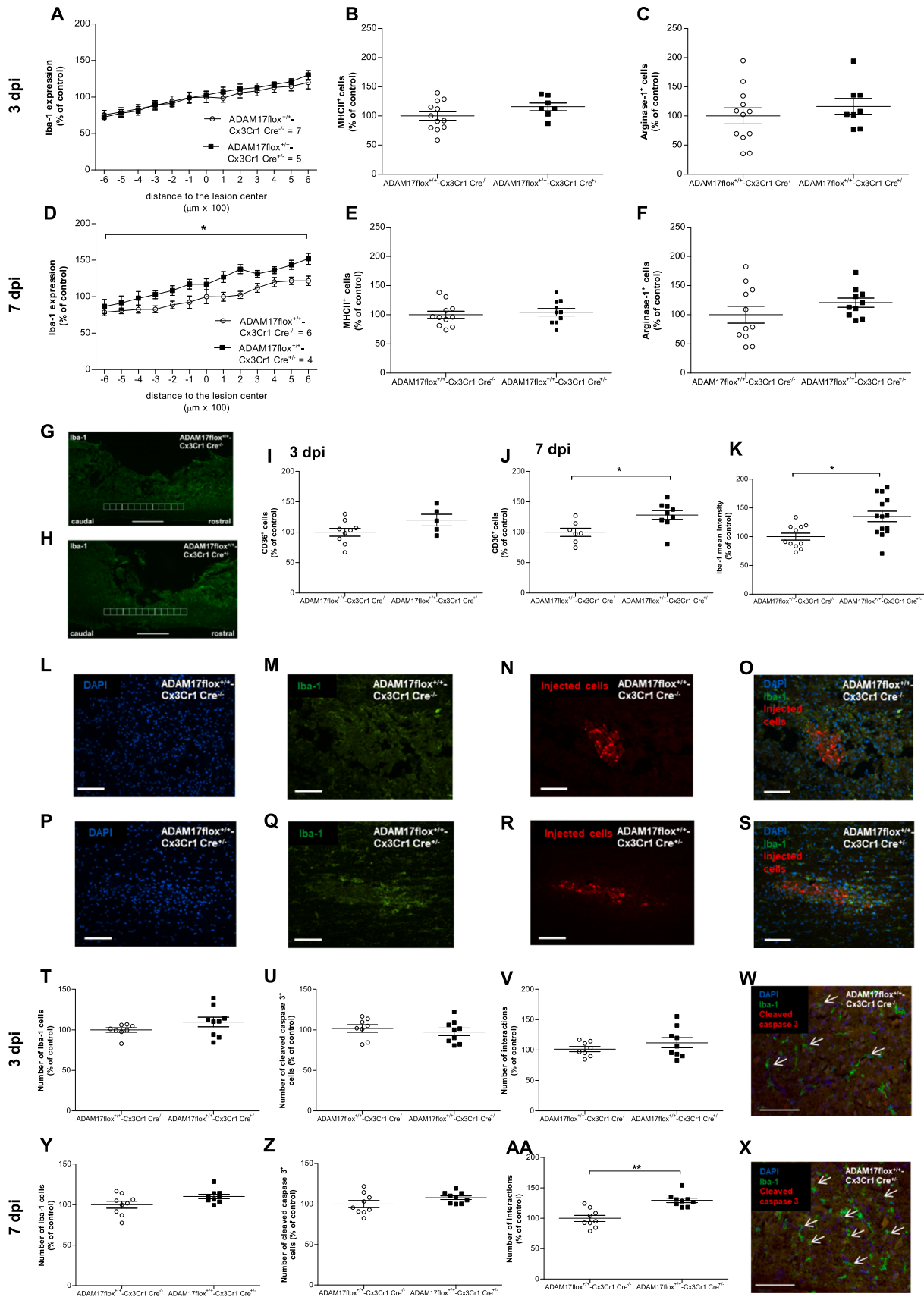
Despite the fact that tissue analysis in ADAM17<sup>ex/ex</sup> mice at 28 dpi revealed no significant difference in Iba-1 intensity, a significant increase in numbers of TMEM119<sup>+</sup> microglia compared to wild type littermates was observed (Fig. 2O). Thus, we investigated whether microglia-specific ADAM17-deficiency results in an improved functional recovery after SCI. To assess the effect of microglial-specific ADAM17-deficiency *in vivo*, ADAM17<sup>+/+</sup> mice were crossed with Cx3Cr1 CreERT2 transgenic mice expressing Cre-recombinase under a tamoxifen-inducible Cx3Cr1 promoter, a promoter expressed in monocytes, monocyte-derived macrophages, tissue-specific macrophages and microglia (Wolf et al., 2013; Yona et al., 2013). This model allows microglia-specific targeting due to the longevity and self-renewal of microglia cells compared to monocytes and monocyte-derived macrophages (Goldmann et al., 2013).

The knockdown efficiency of ADAM17 in ADAM17<sup>+/+</sup>-Cx3Cr1 Cre<sup>+/-</sup> mice after tamoxifen-induced Cre-recombinase expression was confirmed at mRNA (Fig. 5A) and protein level (Fig. 5B). To investigate the effect of microglia-specific ADAM17-deficiency on functional recovery after SCI, an *in vivo* experiment was performed with ADAM17<sup>+/+</sup>-Cx3Cr1 Cre<sup>+/-</sup> and ADAM17<sup>+/+</sup>-Cx3Cr1 Cre<sup>-/-</sup> mice (Fig. 5C). ADAM17<sup>+/+</sup>-Cx3Cr1 Cre<sup>+/-</sup> mice displayed a significantly improved functional recovery from day 8 onwards until the end of the observation period compared to ADAM17<sup>+/+</sup>-Cx3Cr1 Cre<sup>-/-</sup> mice (Fig. 5D), which was similar as the improvement seen in ADAM17<sup>ex/ex</sup> mice (Fig. 2E).

Histological analysis of demyelinated area, lesion size and astrogliosis (Fig. 5E–G) revealed no differences between the 2 groups. When comparing Iba-1 intensity in ADAM17<sup>+/+</sup>-Cx3Cr1 Cre<sup>+/-</sup> with ADAM17<sup>+/+</sup>-Cx3Cr1 Cre<sup>-/-</sup> mice, there was a trend towards a decrease in microglia/macrophage numbers (Fig. 5H–J). In addition, there was a significant reduction in the number of MHCII<sup>+</sup> cells in ADAM17<sup>+/+</sup>-Cx3Cr1 Cre<sup>+/-</sup> compared with ADAM17<sup>+/+</sup>-Cx3Cr1 Cre<sup>-/-</sup> mice (Fig. 5K–M), while no difference in the number of Arginase-1<sup>+</sup> cells (Fig. 5N). In contrast to results of tissue analysis in ADAM17<sup>ex/ex</sup> mice, there were no differences in CD4<sup>+</sup> T (Fig. 5O) and TMEM119<sup>+</sup> cells (Fig. 5P) between the 2 groups. Similarly to results in ADAM17<sup>ex/ex</sup> mice, there was a trend towards a higher ratio of 5-HT<sup>+</sup> fibers in ADAM17<sup>+/+</sup>-Cx3Cr1 Cre<sup>+/-</sup> compared to ADAM17<sup>+/+</sup>-Cx3Cr1 Cre<sup>-/-</sup> mice (Fig. 5Q–S). We further investigated whether microglia-specific ADAM17-deficiency affects axonal dieback and counted therefore the number of microglia/macrophage-axon interactions using Iba-1 and neurofilament staining (supplementary Fig. S2B). No difference in the number of microglia/macrophage-axon contacts between ADAM17<sup>+/+</sup>-Cx3Cr1 Cre<sup>+/-</sup> and ADAM17<sup>+/+</sup>-Cx3Cr1 Cre<sup>-/-</sup> mice was observed. Overall, these data support the hypothesis that specific ADAM17-deficiency on microglia (but not on macrophages or endothelial cells) significantly improves functional recovery after SCI.

### 3.6. Microglia-specific ADAM17-deficiency improves Iba-1-apoptotic cell interactions after SCI

The data provided so far indicate that ADAM17-deficiency leads to an increased expression of the phagocytic receptor CD36 and a better interaction of microglia/macrophages with apoptotic cells. Thus, we further investigated these observations in the ADAM17<sup>+/+</sup>-Cx3Cr1 Cre<sup>+/-</sup> mouse model. Intensity analysis revealed a significant increase of Iba-1<sup>+</sup> microglia/macrophages at 7 dpi in ADAM17<sup>+/+</sup>-Cx3Cr1 Cre<sup>+/-</sup> compared to control mice (Fig. 6A, D, G–H). No significant differences in the number of MHCII<sup>+</sup> and Arginase-1<sup>+</sup> cells between the 2 groups were found (Fig. 6B–C, E–F). Numbers of CD36<sup>+</sup> microglia/macrophages were slightly increased at 3 dpi (Fig. 6I). However, there were significantly higher numbers of CD36<sup>+</sup> microglia/macrophages present at 7 dpi in ADAM17<sup>+/+</sup>-Cx3Cr1 Cre<sup>+/-</sup> compared to ADAM17<sup>+/+</sup>-Cx3Cr1 Cre<sup>-/-</sup> mice (Fig. 6J). To further investigate whether microglial-specific ADAM17-deficiency affects migration and phagocytosis, we injected apoptotic neurons into the spinal cord of



(caption on next page)

**Fig. 6.** Microglia-specific ADAM17-deficiency increases CD36 expression levels and increases the number of cellular interactions between Iba-1<sup>+</sup> microglia/macrophages and apoptotic cells after SCI. Quantification of (A, D) microglia/macrophages, (B, E) MHCII<sup>+</sup> cells and (C, F) Arginase-1<sup>+</sup> cells in spinal cord tissue isolated at 3 and 7 dpi. n = 5–12/group of 2 independent experiments, \*p < 0.05 vs ADAM17<sup>+/+</sup>-Cx3Cr1 Cre<sup>-/-</sup>; two-way ANOVA with a Bonferroni *post-hoc* test. (G, H) Representative images of Iba-1 stained spinal cord sections for ADAM17<sup>+/+</sup>-Cx3Cr1 Cre<sup>-/-</sup> mice and ADAM17<sup>+/+</sup>-Cx3Cr1 Cre<sup>+/-</sup> mice 7 dpi. Scale bars represent 500 μm. (I–J) Quantification and representative images of CD36<sup>+</sup> cells in spinal cord sections at 3 and 7 dpi. n = 5–9/group. \*p < 0.05, Mann Whitney U test. Graph bars represent SEM. (K–S) Quantification and representative images of Iba-1 intensity at the injection site of PKH26-labelled apoptotic cells in ADAM17<sup>+/+</sup>-Cx3Cr1 Cre<sup>-/-</sup> and ADAM17<sup>+/+</sup>-Cx3Cr1 Cre<sup>+/-</sup> mice. Scale bars represent 100 μm. n = 11–14/injection site per group, \*p < 0.05 vs ADAM17<sup>+/+</sup>-Cx3Cr1 Cre<sup>-/-</sup>; Mann Whitney U test. Data are shown as mean ± SEM. Quantification of (T, Y) microglia/macrophages and (U, Z) cleaved caspase 3<sup>+</sup> cells in spinal cord tissue isolated at 3 and 7 dpi. (V, W, X, AA) Quantification and representative images of microglia/macrophage-cleaved caspase 3 interactions at 3 and 7 dpi. Scale bars represent 100 μm. n = 8–9/group of 2 independent experiments. \*p < 0.05 vs ADAM17<sup>+/+</sup>-Cx3Cr1 Cre<sup>-/-</sup>; Mann Whitney U test. Data are shown as mean ± SEM.

uninjured ADAM17<sup>+/+</sup>-Cx3Cr1 Cre<sup>+/-</sup> mice and wild type littermates. Histological analysis revealed a significantly higher Iba-1 intensity at the injection site of ADAM17<sup>+/+</sup>-Cx3Cr1 Cre<sup>+/-</sup> mice compared to ADAM17<sup>+/+</sup>-Cx3Cr1 Cre<sup>-/-</sup> mice (Fig. 6K–S). Equal numbers of microglia/macrophages and cleaved caspase 3<sup>+</sup> cells were determined in both groups, respectively, at 3 and 7 dpi (Fig. 6T–V, Y–AA). Microglia/macrophage interactions with apoptotic cells were significantly increased at 7 dpi in spinal cord sections of ADAM17<sup>+/+</sup>-Cx3Cr1 Cre<sup>+/-</sup> compared to ADAM17<sup>+/+</sup>-Cx3Cr1 Cre<sup>-/-</sup> mice (Fig. 6V–X, AA). These results indicate that ADAM17-deficiency on microglia upregulates CD36 expression and enhances the clearance of apoptotic cells.

#### 4. Discussion

In this study, we demonstrate for the first time that the absence of ADAM17 specifically on microglia, but not macrophages or endothelial cells, promotes phagocytosis and improves histological and functional recovery after SCI in mice. We have used 4 different genetically modified mouse lines as well as bone marrow chimera to demonstrate *in vivo* that microglial ADAM17 plays a detrimental role in the inflammatory and regenerative processes after SCI.

Only a few studies investigated so far the role of ADAM17 in neuroinflammatory pathologies such as traumatic brain injury and multiple sclerosis (Geribaldi-Doldán et al., 2018; Katakowski et al., 2007; Plumb et al., 2006; Zunke and Rose-John, 2017). The role of ADAM17 in SCI is still elusive and until now only studied using rather broad acting pharmacological inhibitors (Vidal et al., 2013; Wei et al., 2015). ADAM10 and ADAM17 are closely related sheddases within the ADAM family. Both sheddases play an essential role in a number of physiological and regenerative processes (Saftig and Reiss, 2011; Zunke and Rose-John, 2017). Interestingly, our results using specific and selective pharmacological inhibitors for ADAM10 and ADAM17 demonstrate that both enzymes affect the pro-inflammatory environment after CNS injury, whereas only ADAM17 plays an essential role in functional recovery after SCI. We further confirmed these data by using the hypomorphic ADAM17 knockin mouse model with a reduction of ADAM17 protein levels in all tissues (Chalaris et al., 2010). In the present study, ADAM17<sup>ex/ex</sup> mice showed a better regeneration of serotonergic fibers and a better functional recovery after SCI. As expected, the demyelinated area was increased in ADAM17<sup>ex/ex</sup> mice due to the important role of ADAM17 in the maturation of oligodendrocyte precursor cells (Palazuelos et al., 2015).

One important function of ADAM17 is the shedding of pro-inflammatory mediators such as TNFα, IL-6R or IL-1R from the plasma membrane. We show that upon ADAM17-deficiency, the pro-inflammatory response is attenuated after SCI, as the number of MHCII<sup>+</sup> cells (interpreted as *classically activated* microglia/macrophages) is reduced. Whereas the number of TMEM119<sup>+</sup> microglia and CD4<sup>+</sup> T cells is increased upon ADAM17-deficiency. The specific subtype of the CD4<sup>+</sup> T cells is unclear. Specific T cell phenotyping after CNS trauma is highly challenging and is prone to artifacts due to the relatively low number of T cells present in the CNS (Beck et al., 2010; Hendrix et al., 2013). Corroborated by others, ADAM17-deficiency or inhibition appears to reduce the number of *classically activated* microglia or

macrophages in the CNS, whereas no changes in the number of *alternatively activated* macrophages have been observed (Hurtado et al., 2002; Madrigal et al., 2002). In contrast to the study by Vidal et al., no differences in lesion size or Iba-1 expression were determined between ADAM17<sup>ex/ex</sup> and wild type mice (Vidal et al., 2013). Furthermore, given that we did not observe differences in Iba-1 expression and lesion size with our specific and selective pharmacological ADAM10/ADAM17 inhibitors, we assume that this discrepancy may be a result of off-target effects of the pharmacological inhibitor.

The clearance of apoptotic cells is essential to resolve inflammation and to prevent further tissue damage (Neumann et al., 2009). Among the different phagocytic receptors, only CD36 was found up-regulated in ADAM17<sup>ex/ex</sup> mice following SCI. Together with the increased interaction between professional phagocytes and apoptotic cells in ADAM17<sup>ex/ex</sup> mice, our results are consistent with previous studies showing that ADAM17-mediated shedding of phagocytic receptors is impairing the resolution of inflammation by affecting the phagocytic behavior of professional phagocytes (Driscoll et al., 2013; Thorp et al., 2011).

The improved functional recovery observed in ADAM17<sup>ex/ex</sup> compared to wild type mice began in the sub-acute phase after SCI. Based on this, it is tempting to speculate that ADAM17-deficiency affects processes taking place during the acute and sub-acute period after SCI. This is further corroborated by the fact that high amounts of soluble TNFα are almost immediately released upon CNS injury leading to a cascade of cellular dysfunctions and excessive inflammatory processes (Pineau and Lacroix, 2007; Takahashi et al., 2003).

In the present study, we show a reduction in TNFα in spinal cord homogenates of ADAM17<sup>ex/ex</sup> mice at 3 dpi, which may be correlated with reduced inflammation in the (sub-) acute phase following SCI. As expected, TNFα levels reduced to baseline in spinal cord homogenates at 7 dpi. Thereby, no difference between ADAM17<sup>ex/ex</sup> mice and wild type controls was observed (Nelissen et al., 2014). Transmembrane and soluble TNFα have distinct effects. Transmembrane TNFα is preferentially signaling via TNFR2 and is regulating gene expression associated among others with cellular survival and resolution of inflammation. Soluble TNFα is preferentially signaling via TNFR1 and has neurotoxic effects, influences the blood-brain permeability as well as neuronal plasticity and is therefore a mediator of neuronal damage and neuropathologies (Olmos and Lladó, 2014).

ADAM17 is the major sheddase of numerous substrates involved in inflammatory responses such as TNFα, IL-6R and others (Zunke and Rose-John, 2017). It is tempting to speculate that ADAM17 influences, due to the release of its substrates, the activation state of macrophages and microglia. This is further based on studies showing that IL-6 signaling through membrane-bound IL-6R is required for differentiation of macrophages into an *alternatively activated* state (Guerrero et al., 2012; Mauer et al., 2014). In contrast to our expectations, our *in vitro* results indicate that the release of ADAM17 substrates from macrophages and microglia cells has no strong effect on their activation state.

Since ADAM17 is expressed on various cell types, we aimed to identify whether ADAM17-deficiency on a specific cell type is affecting inflammation and regeneration after SCI. Therefore, we conditionally inactivated ADAM17.

Adhesion molecules play an essential role in the blood brain/spinal

cord barrier and can influence inflammation and the infiltration of peripheral cells into the CNS (Ma et al., 2013). Additionally, endothelial ADAM17 affects inflammation and barrier integrity (Dreymueller et al., 2012). Data from our endothelial-specific ADAM17-knockout mice show that loss of ADAM17 on endothelial cells does not affect the inflammatory milieu or functional recovery after SCI. Monocyte-derived macrophages start to infiltrate the injured area at 3 dpi and reach their highest activity at 7–10 dpi (David et al., 2015). ADAM17 on myeloid cells is playing an essential role in inflammation and the resolution of inflammation in the periphery (Bell et al., 2007; Horiuchi et al., 2007). No difference in functional recovery in myeloid-specific ADAM17-deficient mice was observed. We observed a significant reduction in lesion size in C57BL/6 ex/ex mice compared to C57BL/6 wt/wt mice. However, there is no clear correlation between lesion size and functional recovery (Inman and Steward, 2003). Lesion size is only one of several factors, which can influence the functional recovery after SCI. As shown by Driscoll and colleagues, ADAM17-deficient macrophages display a better resolution of apoptotic cells *in vivo* (Driscoll et al., 2013). Thereby, it can be speculated that ADAM17-deficiency on macrophages may have led to a better clearance of inflammatory and inhibitory factors, thereby to reduced tissue loss and a reduction in lesion size *in vivo*. Our data demonstrated that ADAM17 expression on infiltrating myeloid cells does not affect the inflammatory environment or functional recovery after SCI.

In ADAM17<sup>ex/ex</sup> mice, a higher number of TMEM119<sup>+</sup> microglia cells was observed in spinal cord tissue at 28 dpi. Consequently, we hypothesized that ADAM17-deficiency affects microglia cells and further investigated this using an inducible microglia-specific ADAM17-knockout mouse model. Microglia-specific ADAM17-deficient mice displayed significantly more fiber regeneration compared to control mice after SCI. Axon regrowth is a prerequisite for functional recovery after SCI. Major obstacles for axonal regrowth following SCI are among others environmental factors such as glial scar, axonal dieback and inhibitory cellular debris (Filous and Schwab, 2018). We did not observe differences in astrogliosis in the hypomorphic ADAM17 mouse model and the microglia-specific ADAM17-deficient mouse model; therefore, it is feasible to speculate that ADAM17-deficiency exerts its beneficial effects not via the modulation of the glial scar. The lengthy retraction of damaged axons from the injury site is known as axonal dieback. Together with the significantly fewer *classically activated* microglia/macrophages observed at 28 dpi, it was tempting to speculate that ADAM17-deficiency might affect microglia/macrophage-induced axonal dieback (Dooley et al., 2016; Evans et al., 2014). In contrast to our expectations, ADAM17-deficiency did not alter the number of microglia/macrophage-axon contacts following SCI. Myelin and cellular debris are obstacles for remyelination and neurite outgrowth as well as axonal regeneration (Kotter et al., 2006; Kottis et al., 2002). In both, ADAM17<sup>ex/ex</sup> and microglia-specific ADAM17 knockout mice, the observed higher expression of CD36 and larger number of microglia/macrophage interactions with apoptotic cells, suggest an improved clearance of apoptotic cells compared to controls. This in turn may have reduced the levels of inhibitory factors, resulting in improved histopathological and functional outcome. *In vitro* phagocytosis assays are known to have several shortcomings among other due the missing variety of stimuli influencing the phagocytic capacity of microglia and monocyte-derived macrophages *in vivo* (Hellwig et al., 2013). Keeping these limitations in mind, our *in vitro* data support the hypothesis that ADAM17-deficiency on microglia and monocyte-derived macrophages influences their phagocytic capacity.

In summary, in this study we show for the first time that ADAM17-deficiency specifically on microglial cells (but not on macrophages or endothelial cells) promotes histological and functional recovery after SCI in mice. Unexpectedly, ADAM17 does not substantially alter the macrophage/microglia phenotype (Cabron et al., 2018). Increased expression of the phagocytic receptor CD36 and a higher number of interactions between microglia/macrophages and apoptotic cells suggest

an increase in phagocytic activity. These data combined with higher numbers of spared, sprouting or regenerating serotonergic fibers in ADAM17<sup>ex/ex</sup> mice (and a trend in microglia-specific ADAM17-deficient mice), may suggest a greater clearance of apoptotic bodies as well as other noxious factors, thereby reducing inflammation. It can be speculated that a less inflammatory milieu promotes regeneration of serotonergic fibers and consequently functional recovery after SCI. Taken together, these data provide first evidence that microglial ADAM17 plays a key role in post-SCI inflammation and exerts detrimental effects on functional and histological recovery after SCI.

## Acknowledgements

The authors thank Prof. Dr. Erik Boddeke (University of Groningen) for his advice and Dr. Leen Timmermans (Hasselt University) for help with the immunohistochemistry. This study was supported by Fonds voor Wetenschappelijk Onderzoek Vlaanderen (FWO; GOA1413, GOA5813FWO, GO6677 to SH and 11ZQ5.16N to DS). The work of SRJ was supported by the Deutsche Forschungsgemeinschaft (Bonn, Germany) Grant CRC877 (Project A1, and the German Cluster of Excellence 306, 'Inflammation at Interfaces').

## Author contributions

DS participated in the study design, *in vivo* and *in vitro* experiments, collection and assembly of data as well as data analysis and manuscript writing. IC participated in the immunohistochemistry and the quantitative image analysis. SS and SL helped with performing *in vivo* experiments and the collection of data. JVB participated in *in vitro* and *in vivo* experiments. DD and PMV helped with surgical procedures and participated in data interpretation. JB and TV carried out the bone marrow transplantation experiment. SRJ participated in the study conception, in data interpretation, in furnishing different mouse lines and in manuscript writing. MGF was involved in the study design and in *in vivo* experiments. SH supervised experiments, participated in the design and coordination of the study and helped to draft the final manuscript. All authors read and approved the final version of the manuscript.

## Conflict of interests

All authors declare that they have no conflict of interest.

## Appendix A. Supplementary data

Supplementary data to this article can be found online at <https://doi.org/10.1016/j.bbi.2019.02.032>.

## References

- Abiega, O., Beccari, S., Diaz-Aparicio, I., Nadjar, A., Layé, S., Leyrolle, Q., Gómez-Nicola, D., Domercq, M., Pérez-Samartín, A., Sánchez-Zafra, V., Paris, I., Valero, J., Savage, J.C., Hui, C.W., Tremblay, M., Deudero, J.J., Brewster, A.L., Anderson, A.E., Zaldumbide, L., Galbarriatu, L., Marinas, A., Vivanco, M., Matute, C., Maletic-Savatic, M., Encinas, J.M., Sierra, A., 2016. Neuronal hyperactivity disturbs ATP microgradients, impairs microglial motility, and reduces phagocytic receptor expression triggering apoptosis/microglial phagocytosis uncoupling. *PLoS Biol.* 14 (5) e1002466.
- Basso, D.M., Fisher, L.C., Anderson, A.J., Jakeman, L.B., McTigue, D.M., Popovich, P.G., 2006. Basso Mouse Scale for locomotion detects differences in recovery after spinal cord injury in five common mouse strains. *J. Neurotraum.* 23 (5), 635–659.
- Beattie, M.S., Hermann, G.E., Rogers, R.C., Bresnahan, J.C., 2002. Cell death in models of spinal cord injury. *Prog. Brain Res.* 137, 37–47.
- Beck, K.D., Nguyen, H.X., Galvan, M.D., Salazar, D.L., Woodruff, T.M., Anderson, A.J., 2010. Quantitative analysis of cellular inflammation after traumatic spinal cord injury: evidence for a multiphasic inflammatory response in the acute to chronic environment. *Brain* 133 (Pt 2), 433–447.
- Bell, J.H., Herrera, A.H., Li, Y., Walcheck, B., 2007. Role of ADAM17 in the ectodomain shedding of TNF-alpha and its receptors by neutrophils and macrophages. *J. Leukoc. Biol.* 82 (1), 173–176.

- Boato, F., Hendrix, S., Huelsenbeck, S.C., Hofmann, F., Grosse, G., Djalali, S., Klimaschewski, L., Auer, M., Just, I., Ahnert-Hilger, G., Hölte, M., 2010. C3 peptide enhances recovery from spinal cord injury by improved regenerative growth of descending fiber tracts. *J. Cell Sci.* 123 (Pt 10), 1652–1662.
- Cabron, A.S., El Azzouzi, K., Boss, M., Arnold, P., Schwarz, J., Rosas, M., Dobert, J.P., Pavlenko, E., Schumacher, N., Renné, T., Taylor, P.R., Linder, S., Rose-John, S., Zunke, F., 2018. Structural and functional analyses of the shedding protease ADAM17 in HoxB8-immortalized macrophages and dendritic-like cells. *J. Immunol.*
- Chalaris, A., Adam, N., Sina, C., Rosenstiel, P., Lehmann-Koch, J., Schirmacher, P., Hartmann, D., Cichy, J., Gavrilova, O., Schreiber, S., Jostock, T., Matthews, V., Häslér, R., Becker, C., Neurath, M.F., Reiss, K., Saftig, P., Scheller, J., Rose-John, S., 2010. Critical role of the disintegrin metalloprotease ADAM17 for intestinal inflammation and regeneration in mice. *J. Exp. Med.* 207 (8), 1617–1624.
- Clausen, B.E., Burkhardt, C., Reith, W., Renkawitz, R., Förster, I., 1999. Conditional gene targeting in macrophages and granulocytes using LysMcre mice. *Transg. Res.* 8 (4), 265–277.
- David, S., Greenhalgh, A.D., Kroner, A., 2015. Macrophage and microglial plasticity in the injured spinal cord. *Neuroscience* 307, 311–318.
- Dooley, D., Lemmens, E., Vanganswinkel, T., Le Blon, D., Hoornaert, C., Ponsaerts, P., Hendrix, S., 2016. Cell-based delivery of interleukin-13 directs alternative activation of macrophages resulting in improved functional outcome after spinal cord injury. *Stem Cell Rep.* 7 (6), 1099–1115.
- Dreymueller, D., Ludwig, A., 2017. Considerations on inhibition approaches for proinflammatory functions of ADAM proteases. *Platelets* 28 (4), 354–361.
- Dreymueller, D., Martin, C., Kogel, T., Pruessmeyer, J., Hess, F.M., Horiuchi, K., Uhlig, S., Ludwig, A., 2012. Lung endothelial ADAM17 regulates the acute inflammatory response to lipopolysaccharide. *EMBO Mol. Med.* 4 (5), 412–423.
- Driscoll, W.S., Vaisar, T., Tang, J., Wilson, C.L., Raines, E.W., 2013. Macrophage ADAM17 deficiency augments CD36-dependent apoptotic cell uptake and the linked anti-inflammatory phenotype. *Circ. Res.* 113 (1), 52–61.
- Evans, T.A., Barkauskas, D.S., Myers, J.T., Hare, E.G., You, J.Q., Ransohoff, R.M., Huang, A.Y., Silver, J., 2014. High-resolution intravital imaging reveals that blood-derived macrophages but not resident microglia facilitate secondary axonal dieback in traumatic spinal cord injury. *Exp. Neurol.* 254, 109–120.
- Filous, A.R., Schwab, J.M., 2018. Determinants of axon growth, plasticity, and regeneration in the context of spinal cord injury. *Am. J. Pathol.* 188 (1), 53–62.
- Fu, P.C., Tang, R.H., Wan, Y., Xie, M.J., Wang, W., Luo, X., Yu, Z.Y., 2016. ROCK inhibition with fasudil promotes early functional recovery of spinal cord injury in rats by enhancing microglia phagocytosis. *J. Huazhong Univ. Sci. Technol. Med. Sci.* 36 (1), 31–36.
- Geribaldi-Doldán, N., Carrasco, M., Murillo-Carretero, M., Domínguez-García, S., García-Cózar, F.J., Muñoz-Miranda, J.P., Del Río-García, V., Verástegui, C., Castro, C., 2018. Specific inhibition of ADAM17/TACE promotes neurogenesis in the injured motor cortex. *Cell Death Dis* 9 (9), 862.
- Goldmann, T., Wieghofer, P., Müller, P.F., Wolf, Y., Varol, D., Yona, S., Brendecke, S.M., Kierdorf, K., Staszewski, O., Datta, M., Luedde, T., Heikenwalder, M., Jung, S., Prinz, M., 2013. A new type of microglia gene targeting shows TAK1 to be pivotal in CNS autoimmune inflammation. *Nat. Neurosci.* 16 (11), 1618–1626.
- Graeber, M.B., 2010. Changing face of microglia. *Science* 330 (6005), 783–788.
- Guerrero, A.R., Uchida, K., Nakajima, H., Watanabe, S., Nakamura, M., Johnson, W.E., Baba, H., 2012. Blockade of interleukin-6 signaling inhibits the classic pathway and promotes an alternative pathway of macrophage activation after spinal cord injury in mice. *J. Neuroinflamm.* 9, 40.
- Gyoneva, S., Ransohoff, R.M., 2015. Inflammatory reaction after traumatic brain injury: therapeutic potential of targeting cell-cell communication by chemokines. *Trends Pharmacol. Sci.* 36 (7), 471–480.
- Hellwig, S., Heinrich, A., Biber, K., 2013. The brain's best friend: microglial neurotoxicity revisited. *Front. Cell Neurosci.* 7, 71.
- Hendrix, S., Kramer, P., Pehl, D., Warnke, K., Boato, F., Nelissen, S., Lemmens, E., Pejler, G., Metz, M., Siebenhaar, F., Maurer, M., 2013. Mast cells protect from post-traumatic brain inflammation by the mast cell-specific chymase mouse mast cell protease-4. *FASEB J.* 27 (3), 920–929.
- Horiuchi, K., Kimura, T., Miyamoto, T., Takaishi, H., Okada, Y., Toyama, Y., Blobel, C.P., 2007. Cutting edge: TNF-alpha-converting enzyme (TACE/ADAM17) inactivation in mouse myeloid cells prevents lethality from endotoxin shock. *J. Immunol.* 179 (5), 2686–2689.
- Horn, K.P., Busch, S.A., Hawthorne, A.L., van Rooijen, N., Silver, J., 2008. Another barrier to regeneration in the CNS: activated macrophages induce extensive retraction of dystrophic axons through direct physical interactions. *J. Neurosci.* 28 (38), 9330–9341.
- Hundhausen, C., Misztela, D., Berkhout, T.A., Broadway, N., Saftig, P., Reiss, K., Hartmann, D., Fahrenholz, F., Postina, R., Matthews, V., Kallen, K.J., Rose-John, S., Ludwig, A., 2003. The disintegrin-like metalloprotease ADAM10 is involved in constitutive cleavage of CX3CL1 (fractalkine) and regulates CX3CL1-mediated cell-cell adhesion. *Blood* 102 (4), 1186–1195.
- Hurtado, O., Lizasoain, I., Fernández-Tomé, P., Alvarez-Barrientos, A., Leza, J.C., Lorenzo, P., Moro, M.A., 2002. TACE/ADAM17-TNF-alpha pathway in rat cortical cultures after exposure to oxygen-glucose deprivation or glutamate. *J. Cereb. Blood Flow Metab.* 22 (5), 576–585.
- Inman, D.M., Steward, O., 2003. Physical size does not determine the unique histopathological response seen in the injured mouse spinal cord. *J. Neurotraum.* 20 (1), 33–42.
- Katakowski, M., Chen, J., Zhang, Z.G., Santra, M., Wang, Y., Chopp, M., 2007. Stroke-induced subventricular zone proliferation is promoted by tumor necrosis factor-alpha-converting enzyme protease activity. *J. Cereb. Blood Flow Metab.* 27 (4), 669–678.
- Kotter, M.R., Li, W.W., Zhao, C., Franklin, R.J., 2006. Myelin impairs CNS remyelination by inhibiting oligodendrocyte precursor cell differentiation. *J. Neurosci.* 26 (1), 328–332.
- Kottis, V., Thibault, P., Mikol, D., Xiao, Z.C., Zhang, R., Dergham, P., Braun, P.E., 2002. Oligodendrocyte-myelin glycoprotein (OMgp) is an inhibitor of neurite outgrowth. *J. Neurochem.* 82 (6), 1566–1569.
- Ma, Q., Chen, S., Klebe, D., Zhang, J.H., Tang, J., 2013. Adhesion molecules in CNS disorders: biomarker and therapeutic targets. *CNS Neurol. Disord. Drug Targets* 12 (3), 392–404.
- Madrigal, J.L., Hurtado, O., Moro, M.A., Lizasoain, I., Lorenzo, P., Castellano, A., Boscá, L., Leza, J.C., 2002. The increase in TNF-alpha levels is implicated in NF-kappaB activation and inducible nitric oxide synthase expression in brain cortex after immobilization stress. *Neuropsychopharmacology* 26 (2), 155–163.
- Mauer, J., Chaurasia, B., Goldau, J., Vogt, M.C., Ruud, J., Nguyen, K.D., Theurich, S., Hausen, A.C., Schmitz, J., Brönneke, H.S., Estevez, E., Allen, T.L., Mesaros, A., Partridge, L., Febbraio, M.A., Chawla, A., Wunderlich, F.T., Brüning, J.C., 2014. Signaling by IL-6 promotes alternative activation of macrophages to limit endotoxemia and obesity-associated resistance to insulin. *Nat. Immunol.* 15 (5), 423–430.
- Mazaheri, F., Snaidero, N., Kleinberger, G., Madore, C., Daria, A., Werner, G., Krasemann, S., Capell, A., Trümbach, D., Wurst, W., Brunner, B., Bultmann, S., Tahirovic, S., Kerschenshneider, M., Misgeld, T., Butovsky, O., Haass, C., 2017. TREM2 deficiency impairs chemotaxis and microglial responses to neuronal injury. *EMBO Rep.* 18 (7), 1186–1198.
- Murray, P.J., Wynn, T.A., 2011. Obstacles and opportunities for understanding macrophage polarization. *J. Leukoc. Biol.* 89 (4), 557–563.
- Nelissen, S., Vanganswinkel, T., Geurts, N., Geboes, L., Lemmens, E., Vidal, P.M., Lemmens, S., Willems, L., Boato, F., Dooley, D., Pehl, D., Pejler, G., Maurer, M., Metz, M., Hendrix, S., 2014. Mast cells protect from post-traumatic spinal cord damage in mice by degrading inflammation-associated cytokines via mouse mast cell protease 4. *Neurobiol. Dis.* 62, 260–272.
- Neumann, H., Kotter, M.R., Franklin, R.J., 2009. Debris clearance by microglia: an essential link between degeneration and regeneration. *Brain* 132 (Pt 2), 288–295.
- Nikodemova, M., Watters, J.J., 2012. Efficient isolation of live microglia with preserved phenotypes from adult mouse brain. *J. Neuroinflamm.* 9, 147.
- Olmos, G., Lladó, J., 2014. Tumor necrosis factor alpha: a link between neuroinflammation and excitotoxicity. *Mediat. Inflamm.* 2014 861231.
- Orr, M.B., Gensel, J.C., 2018. Spinal cord injury scarring and inflammation: therapies targeting glial and inflammatory responses. *Neurotherapeutics.*
- Palazuelos, J., Klingener, M., Raines, E.W., Crawford, H.C., Aguirre, A., 2015. Oligodendrocyte regeneration and CNS remyelination require TACE/ADAM17. *J. Neurosci.* 35 (35), 12241–12247.
- Pineau, I., Lacroix, S., 2007. Proinflammatory cytokine synthesis in the injured mouse spinal cord: multiphasic expression pattern and identification of the cell types involved. *J. Comp. Neurol.* 500 (2), 267–285.
- Plumb, J., McQuaid, S., Cross, A.K., Surr, J., Haddock, G., Bunning, R.A., Woodroffe, M.N., 2006. Upregulation of ADAM-17 expression in active lesions in multiple sclerosis. *Mult. Scler.* 12 (4), 375–385.
- Ravichandran, K.S., 2010. Find-me and eat-me signals in apoptotic cell clearance: progress and conundrums. *J. Exp. Med.* 207 (9), 1807–1817.
- Rego, S.L., Helms, R.S., Dréau, D., 2014. Tumor necrosis factor-alpha-converting enzyme activities and tumor-associated macrophages in breast cancer. *Immunol. Res.* 58 (1), 87–100.
- Saftig, P., Reiss, K., 2011. The “A Disintegrin And Metalloproteases” ADAM10 and ADAM17: novel drug targets with therapeutic potential? *Eur. J. Cell Biol.* 90 (6–7), 527–535.
- Takahashi, J.L., Giuliani, F., Power, C., Imai, Y., Yong, V.W., 2003. Interleukin-1beta promotes oligodendrocyte death through glutamate excitotoxicity. *Ann. Neurol.* 53 (5), 588–595.
- Tamashiro, T.T., Dalgard, C.L., Byrnes, K.R., 2012. Primary microglia isolation from mixed glial cell cultures of neonatal rat brain tissue. *J. Vis. Exp.* (66) e3814.
- Thorp, E., Vaisar, R., Subramanian, M., Mautner, L., Blobel, C., Tabas, I., 2011. Shedding of the Mer tyrosine kinase receptor is mediated by ADAM17 protein through a pathway involving reactive oxygen species, protein kinase Cδ, and p38 mitogen-activated protein kinase (MAPK). *J. Biol. Chem.* 286 (38), 33335–33344.
- Vanganswinkel, T., Geurts, N., Quanten, K., Nelissen, S., Lemmens, S., Geboes, L., Dooley, D., Vidal, P.M., Pejler, G., Hendrix, S., 2016. Mast cells promote scar remodeling and functional recovery after spinal cord injury via mouse mast cell protease 6. *FASEB J.* 30 (5), 2040–2057.
- Vidal, P.M., Lemmens, E., Avila, A., Vanganswinkel, T., Chalaris, A., Rose-John, S., Hendrix, S., 2013. ADAM17 is a survival factor for microglial cells in vitro and in vivo after spinal cord injury in mice. *Cell Death Dis.* 4 e954.
- Wagner, B.J., Lindau, D., Ripper, D., Stierhof, Y.D., Glatzle, J., Witte, M., Beck, H., Keppeler, H., Lauber, K., Rammensee, H.G., Königszgraber, A., 2011. Phagocytosis of dying tumor cells by human peritoneal mesothelial cells. *J. Cell. Sci.* 124 (Pt 10), 1644–1654.
- Wang, Y., Nakayama, M., Pitulescu, M.E., Schmidt, T.S., Bochenek, M.L., Sakakibara, A., Adams, S., Davy, A., Deutsch, U., Lüthi, U., Barberis, A., Benjamin, L.E., Mäkinen, T., Nobes, C.D., Adams, R.H., 2010. Ephrin-B2 controls VEGF-induced angiogenesis and lymphangiogenesis. *Nature* 465 (7297), 483–486.
- Wei, Z., Yu, D., Bi, Y., Cao, Y., 2015. A disintegrin and metalloprotease 17 promotes microglial cell survival via epidermal growth factor receptor signalling following spinal cord injury. *Mol. Med. Rep.* 12 (1), 63–70.
- Weinger, J.G., Omari, K.M., Marsden, K., Raine, C.S., Shafiq-Zagardo, B., 2009. Up-regulation of soluble Axl and Mer receptor tyrosine kinases negatively correlates with Gas6 in established multiple sclerosis lesions. *Am. J. Pathol.* 175 (1), 283–293.

- Wolf, Y., Yona, S., Kim, K.W., Jung, S., 2013. Microglia, seen from the CX3CR1 angle. *Front. Cell. Neurosci.* 7, 26.
- Yona, S., Kim, K.W., Wolf, Y., Mildner, A., Varol, D., Breker, M., Strauss-Ayali, D., Viukov, S., Guilliama, M., Misharin, A., Hume, D.A., Perlman, H., Malissen, B., Zelzer, E., Jung, S., 2013. Fate mapping reveals origins and dynamics of monocytes and tissue macrophages under homeostasis. *Immunity* 38 (1), 79–91.
- Zhang, S., Kojic, L., Tsang, M., Grewal, P., Liu, J., Namjoshi, D., Wellington, C.L., Tetzlaff, W., Cynader, M.S., Jia, W., 2016. Distinct roles for metalloproteinases during traumatic brain injury. *Neurochem. Int.* 96, 46–55.
- Zunke, F., Rose-John, S., 2017. The shedding protease ADAM17: Physiology and pathophysiology. *Biochim. Biophys. Acta.*